UNIVERSITY OF CRETE
SCHOOL OF SCIENCES AND ENGINEERING
DEPARTMENT OF MATHEMATICS AND APPLIED MATHEMATICS

Master Thesis

An Iterative Scheme for Estimating the Acoustic Field in Sea Environment with an Elastic Seabed

Ioannis Mastrokalos

Supervisor :
Michael Taroudakis
Professor
Department of Mathematics and Applied Mathematics

Fall 2015

Contents

Abstract **3**

Acknowledgement **4**

1. Introduction **5**

2. The problem of sound propagation in shallow water range-independent waveguide **7**
2.1. The acoustic wave equation 8
2.2. Transmission Loss 9

3. The depth problem **10**
3.1. Constant sound speed profile 11
3.2. Sound speed profile varying with depth 14

4. Estimation of eigenvalues for a sound velocity profile varying with depth **17**
4.1. Inverse Power Iteration 17
4.2. Calculation of the eigenvalues by means of an iterative scheme 18

5. Applications - Results **20**
5.1. Constant sound speed profile 20
5.1.1. When the source frequency is 20 Hz 20
5.1.2. When the source frequency is 40 Hz 24
5.2. Sound speed profile varying with depth 27
5.2.1. Linearly increasing sound speed over a soft elastic bottom 27
5.2.2. Linearly increasing sound speed over a hard elastic bottom 30
5.2.3. Linearly varying sound speed with an alternating monotonicity . . 37

6. Summary - Conclusion **47**

Appendix A. Derivation of pressure field and normalization constant **48**
A.1. Pressure field 48
A.2. Normalization constant 49

Bibliography **51**

Abstract

This work deals with a suggested technique for the calculation of the complex eigenvalues and associated eigenfunctions of the "depth problem", associated with the sound propagation in range-independent shallow water environment over a homogeneous elastic half-space, when the sound speed profile in the water varies with depth. The idea is that the eigenvalues in such an environment can be estimated by means of an iterative procedure, initialized by the Effective-Depth method for a constant sound speed profile. The eigenfunctions are computed numerically by use of the finite-difference approach and, eventually, the computation of the acoustic pressure field is possible in terms of an eigenfunction series. The efficiency of the suggested technique is tested by comparing its results to those obtained by the KRAKEN-C normal mode program.

Περίληψη

Στην παρούσα εργασία παρουσιάζεται μια προτεινόμενη τεχνική για τον υπολογισμό των ιδιοτιμών και ιδιοσυναρτήσεων του προβλήματος βάθους, το οποίο σχετίζεται με την ακουστική διάδοση σε θαλάσσιο κυματοδηγό. Ειδικότερα, ο πυθμένας του περιβάλλοντος θεωρείται ως ένα ελαστικό ημιάπειρο μέσο και η ταχύτητα διάδοσης του ήχου στο νερό μπορεί να μεταβάλλεται με το βάθος, ενώ όλες οι παράμετροι του προβλήματος θεωρούνται ανεξάρτητες ως προς την απόσταση. Η ιδέα είναι ότι οι ιδιοτιμές σε ένα τέτοιο περιβάλλον μπορούν να υπολογισθούν μέσω ενός επαναληπτικού σχήματος για το οποίο οι αρχικές εκτιμήσεις προκύπτουν από τη μέθοδο του Ενεργού Βάθους για σταθερό προφίλ ταχύτητας. Οι ιδιοσυναρτήσεις του προβλήματος υπολογίζονται αριθμητικά με ένα σχήμα πεπερασμένων διαφορών και, τελικά, η ακουστική πίεση μπορεί να αναπτυχθεί σε σειρά ιδιοσυναρτήσεων. Η αποτελεσματικότητα της προτεινόμενης τεχνικής ελέγχεται μέσω συγκρίσεων των αποτελεσμάτων με τα αντίστοιχα που προκύπτουν από το πρόγραμμα KRAKEN-C.

Acknowledgement

This work has been supported by PEFYKA project within the KRIPIS Action of the GSRT. The project is funded by Greece and the European Regional Development Fund of the European Union under the NSRF and the O.P. Competitiveness and Entrepreneurship.

1. Introduction

Since the velocity of sound in the water has appeared to be high enough, acoustics have been proved to be an excellent tool for oceanographic researh. Underwater communication has been achieved by means of acoustic propagation and the localization of underwater objects, either by passive or active acoustic observation, has become possible.

Another topic of acoustics could be the study of undersea seismicity. In our work, we are interested in propagating sound in the water column due to an earthquake, in order to characterize its acoustic signature. Thus, all considerations that will follow concern a water layer laying over a semi-infinite, elastic seabed. The problem is governed by the *Helmholtz* equation in combination with the appropriate boundary conditions and the solution can be expressed as an eigenfuction series expansion.

This work deals with an alternative technique for the calculation of the complex eigenvalues and eigenfunctions associated with the acoustic field in range-independent shallow water environment. In particular, the case of a sound speed profile varying with depth is studied. A finite-difference scheme is employed for the approximation of the partial derivatives of the pressure field with respect to depth, leading to a matrix eigenvalue problem. The eigenvalues are approximated by means of an iterative scheme, based on Inverse Power Iteration, of which the starting values are the eigenvalues of the same problem with constant sound velocity and are obtained using the Effective-Depth method.

Results obtained by this technique are compared to those produced by the KRAKEN-C normal mode program in terms of eigenvalues, eigenfunctions and eventually the acoustic field for typical sandy underwater environments. Several test cases are considered concerning various environmental parameters, including the shear wave speed in the bottom, the sound speed profile in the water column and the source frequency.

Outline of the thesis

In chapter 2 a description of the undersea environment is given with the characteristic parameters in the water layer and the seabed. The wave equation for the acoustic pressure field is expressed in linear form and seperation of the spatial variables from time leads to the *Helmholtz* equation. Application of the appropriate boundary conditions results in a well defined problem of which the solution is given in eigenfuction series expansion. Last the transmission loss, which is of great interest, is defined. In chapter 3 the eigenfunctions, by means of which the pressure field is expressed, are defined in terms of a boundary value problem called the "depth problem". The cases of a constant and a varying with depth sound speed profile are studied seperately. Refering to the former case the Effective-Depth approach, for the computation of the eigenvalues, is described in short and the associated eigenfuctions are expressed explicitly. The latter case is studied in depth. A finite difference scheme is used and discrete values of the eigenfunctions appear to satisfy a matrix eigenvalue problem. For the estimation of the associated eigenvalues, an iterative procedure described extensively in chapter 4 is suggested. Chapter 5 concerns applications and results obtained by both the effective depth and the suggested iterative scheme. Validity of these results is tested by comparison to the output of the KRAKEN-C program. Eventually, in chapter 6 a summary of the thesis is presented with the corresponding conclusions and suggestions for future researh.

2. The problem of sound propagation in shallow water range-independent waveguide

In this chapter the problem of underwater sound propagation is formulated under the consideration of a range-independed environment. The solution is given by means of the normal mode approximation and the transmission loss, which is the main measurement in acoustic propagation problems, is defined.

The sea environment is represented in the cylindrical coordinates system (r, ϕ, z) with

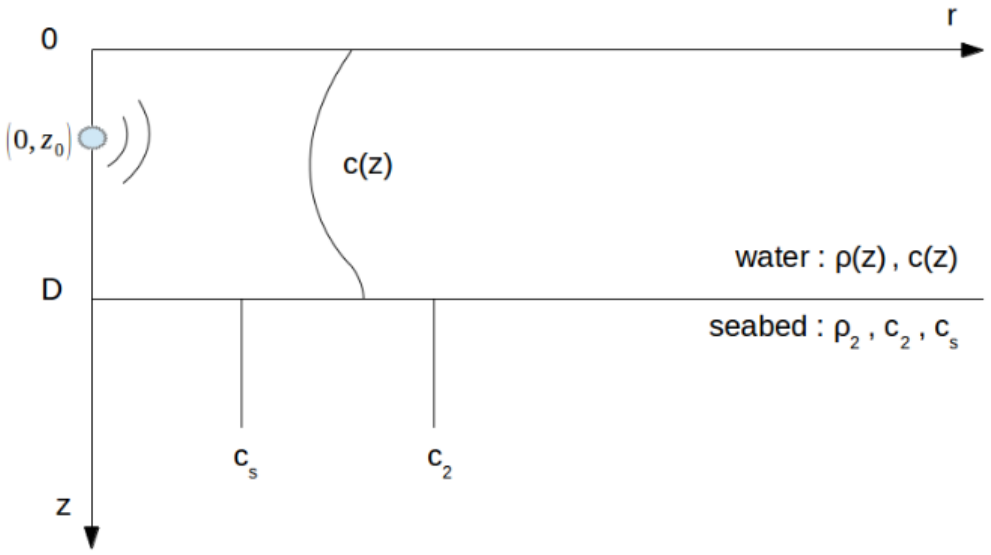

Figure 2.1.: Schematic representation of the underwater environment with the corresponding parameters

axial symmetry with respect to the z-axis. That is, there is no dependence on the angle ϕ and the representation can be reduced into two dimensions (r, z). We consider a water layer laying over an elastic seabed which is represented as a semi-infinite halfspace. The air-water and water-seabed interfaces are considered plane and horizontal at depths $z = 0$ and $z = D$ respectively and z-axis is positive downward as shown in figure (2.1). A monochromatic point source of frequency f is located at the point $(0, z_0)$ and the parameters in the water are the density of the water $\rho(z)$ and the velocity of sound

propagation $c(z)$ which may vary only with depth. The parameters in the seabed are the density of the seabed ρ_2, the velocity of compessional waves c_2 and the velocity of shear waves c_s which are considered constant.

2.1. The acoustic wave equation

We are interested in computing the acoustic pressure governed by the acoustic wave equation

$$\nabla\left(\frac{1}{\rho(z)}\nabla P\right) - \frac{1}{\rho(z)c(z)^2}P_{tt} = -s(t)\frac{\delta(z-z_0)\delta(r)}{2\pi r} \tag{2.1}$$

where P indicates the acoustic pressure field and is a function of the spatial coordinates and time (r, z, t). The right-hand side of eq. 2.1 indicates the presence of the source within the domain of study and the time dependence of the source is described by the function $s(t)$. Having considered a monochromatic point source of unit strength with angular frequency $\omega = 2\pi f$, we can assume that $s(t) = e^{-i\omega t}$ thus we have for the acoustic pressure

$$P(r, z, t) = p(r, z)e^{-i\omega t}$$

Substituting the above expression into eq. 2.1 we get the well known *Helmholtz* equation in cylindrical coordinates with axial symmetry

$$\frac{1}{r}\frac{\partial}{\partial r}\left(r\frac{\partial p}{\partial r}\right) + \rho(z)\frac{\partial}{\partial z}\left(\frac{1}{\rho(z)}\frac{\partial p}{\partial z}\right) + \frac{\omega^2}{c^2(z)}p = -\frac{\delta(z-z_0)\delta(r)}{2\pi r} \tag{2.2}$$

which in combination with the boundary conditions of a pressure release air-water interface, an appropriate impedance condition at the water-seabed interface and a Sommerfeld radiation condition for the behaviour of the pressure field while $r \to \infty$ defines a well posed boundary value problem. The surface and impedance conditions are formulated as

$$p(\cdot, 0) = 0 \tag{2.3}$$

$$p(\cdot, D) + I(\lambda)\frac{\partial p(\cdot, D)}{\partial z} = 0 \tag{2.4}$$

where $I(\lambda)$ is called the impedance function and depends on a parameter λ which will be discussed later.

The solution to problem (2.2)-(2.4) can be expressed in eigenfunction series expansion as

$$p(r, z) = \sum_n A_n(r)u_n(z) \tag{2.5}$$

where the functions A_n indicate the range dependence of the pressure field and u_n are the eigenfunctions of the "depth problem" defined and studied in depth in chapter 3,

indicating the depth dependence. According to the present bibliography ([1, 4, 5]), the final expression for the solution is given as

$$p(r,z) = \frac{i}{4}\sum_{n} u_n(z_0)u_n(z)H_0^{(1)}(\lambda_n r) \tag{2.6}$$

where the function $H_0^{(1)}(\cdot)$ is a *Hankel* function of the first kind of zeroth order. The argument λ_n of the *Hankel* function is directly related to the parameter λ above and is discussed in the next chapter. Since we are interested in sound propagation at a great distance, the asymptotic expression of the *Hankel* function is used. That is

$$H_0^{(1)}(\lambda_n r) = \sqrt{\frac{2}{\pi\lambda_n r}}e^{i(\lambda_n r - \pi/4)} \tag{2.7}$$

It is noted that a short description of the derivation of expression 2.6 is included in appendix A.

2.2. Transmission Loss

When doing acoustics, one is actually interested in computing the transmission loss defined as

$$TL(r,z) = -20\log\frac{|p(r,z)|}{|p_0|} \tag{2.8}$$

where p_0 is a reference pressure defined as the pressure at 1 m distance from a point source which emits in free space. The reference pressure p_0 is derived by the solution p_{sph} of the *Helmholtz* equation in spherical coordinates with spherical symmetry, under the condition of a diverging wave. That is,

$$p_{sph}(r) = \frac{1}{4\pi r}e^{i\frac{\omega}{c}r} \tag{2.9}$$

Thus,

$$|p_0| = \frac{1}{4\pi} \tag{2.10}$$

and (2.8) becomes

$$TL(r,z) = -20\log|4\pi p(r,z)| \tag{2.11}$$

3. The depth problem

In this chapter the "depth problem" is defined and solved for two different cases: a) when the environmental parameters are constant and b) when they vary with depth. In case a) the effective depth approach will be presented in short. In case b) the only parameter considered as varying with depth is the sound velocity $c(z)$ whereas the density of the water $\rho(z)$ will be considered as constant.

The depth problem is defined as follows: Compute pairs $(\lambda_n, u_n(z))$ such that

$$\rho(z)\frac{d}{dz}\left(\frac{1}{\rho(z)}\frac{du_n}{dz}\right) + (k^2(z) - \lambda_n^2)u_n = 0 \ , \ z \in [0, D] \tag{3.1}$$

$$u_n(0) = 0 \tag{3.2}$$

$$\frac{u_n(D)}{u_n'(D)} = I(\lambda_n) \tag{3.3}$$

where $k(z) = \frac{\omega}{c(z)}$ is the wavenumber. The above problem is an eigenvalue/eigenfunction problem where λ_n is the eigenvalue associated with the eigenfunction u_n and, since we are interested in computing the pressure field in the water column, its domain is the interval $[0, D]$. Equations (3.2) and (3.3) correspond to a pressure release sea surface and an appropriate impedance condition respectively. The impedance condition is defined through the impedance function $I(\lambda_n)$ which relates the value of an eigenfunction at depth $z = D$ to its first derivative at the same depth and includes information about the influence of the seabed on the pressure field in the water column.

Since in both cases a) and b) the water density is considered constant, problem (3.1)-(3.3) is reduced to

$$\frac{d^2u_n}{dz^2} + (k^2(z) - \lambda_n^2)u_n = 0 \ , \ z \in [0, D] \tag{3.4}$$

under the same boundary conditions.

In order to proceed with giving the solution of the depth problem {(3.4),(3.2),(3.3)} we need to define the plane wave reflection coefficient between a fluid and a solid medium $R(\lambda)$.

$$R(\lambda) = \frac{4\gamma_2\delta_2\lambda^2 + (\delta_2^2 - \lambda^2)^2 - \left(\frac{\rho}{\rho_2}\frac{\gamma_2}{\gamma}\frac{\omega^4}{c_s^4}\right)}{4\gamma_2\delta_2\lambda^2 + (\delta_2^2 - \lambda^2)^2 + \left(\frac{\rho}{\rho_2}\frac{\gamma_2}{\gamma}\frac{\omega^4}{c_s^4}\right)} \tag{3.5}$$

where

$$\gamma = \sqrt{k^2 - \lambda^2}$$
$$\gamma_2 = \sqrt{\frac{\omega^2}{c_2^2} - \lambda^2}$$
$$\delta_2 = \sqrt{\frac{\omega^2}{c_s^2} - \lambda^2}$$

denote the vertical component of the wavenumbers $k(z)$, $k_2 = \frac{\omega}{c_2}$ and $k_s = \frac{\omega}{c_s}$ of sound waves in the water column, compressional waves in the seabed and shear waves in the seabed respectively.

3.1. Constant sound speed profile

In case the sound speed profile is constant the wavenumber has no dependence on z, that is $k(z) = k$ and if one defines $\gamma_n = \sqrt{k^2 - \lambda_n^2}$ $(n = 1, 2, \dots)$, the general solution of (3.4) is given in terms of complex exponentials as

$$u_n(z) = A_n e^{i\gamma_n z} + B_n e^{-i\gamma_n z} \tag{3.6}$$

where the first term indicates waves propagating downward and the second waves propagating upward. The coefficients A_n, B_n are constant and depend on the eigenpair (λ_n, u_n). Applying boundary condition (3.2) on the solution (3.6) gives

$$\begin{aligned} u_n(0) &= 0 \\ \Rightarrow A_n &= -B_n \end{aligned} \tag{3.7}$$

and substituting this result into (3.6) one gets

$$\begin{aligned} u_n(z) &= A_n(e^{i\gamma_n z} - e^{-i\gamma_n z}) \\ \Rightarrow u_n(z) &= i2A_n \sin(\gamma_n z) \end{aligned} \tag{3.8}$$

where the coefficient A_n needs to be determined as well as the corresponding eigenvalue λ_n. Note that close to the seabed the solution (3.6) can be expressed in terms of the reflection coefficient $R(\lambda_n)$ as

$$u_n(z) = C_n(e^{-i\gamma_n(D-z)} + R(\lambda_n)e^{i\gamma_n(D-z)}) \tag{3.9}$$

Now if we apply (3.3) to (3.9) we get an expression for the impedance function, that is

$$I(\lambda_n) = \frac{(1 + R(\lambda_n))}{i\gamma_n(1 - R(\lambda_n))} \tag{3.10}$$

and if we apply (3.3) to (3.8) we get a second expression as

$$\begin{aligned} I(\lambda_n) &= \frac{\sin \gamma_n D}{\gamma_n \cos \gamma_n D} \\ &= \frac{\tan \gamma_n D}{\gamma_n} \end{aligned} \tag{3.11}$$

So from (3.10) and (3.11) we demand

$$\tan \gamma_n D = \frac{(1 + R(\lambda_n))}{i(1 - R(\lambda_n))} \tag{3.12}$$

That is, λ_n is an eigenvalue of the depth problem *if and only if* it satisfies (3.12). Consequently, for the case with a constant sound speed profile, the eigenvalues can be computed by solving for the roots of the function corresponding to eq.(3.12) which is a non-linear and in general complex function.

In previous works several techniques have been applied on solving for the complex roots of eq. (3.12). Some of these techniques are

- systematic search on the complex plane [8]
- root finder techniques [2]
- effective depth method [4]

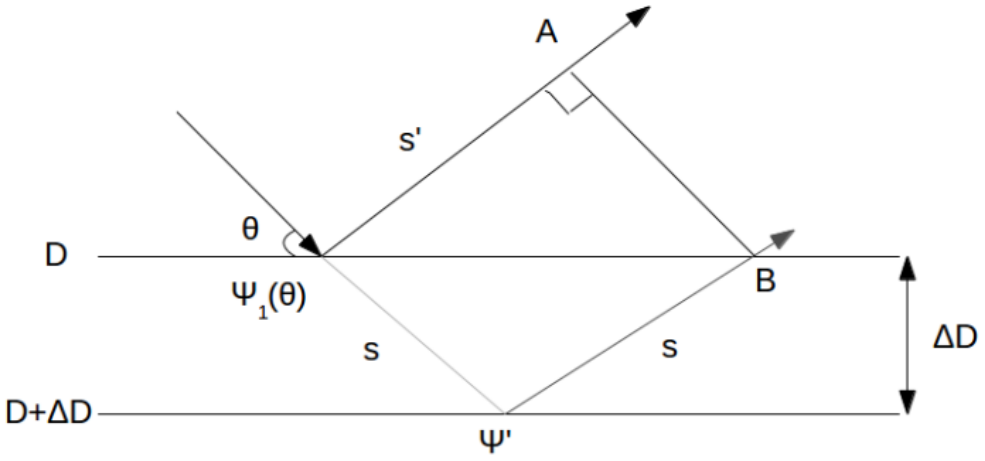

Figure 3.1.: Geometry of the effective-depth

Since the complex effective depth method will be used as a first step for computing the eigenvalues in the case of a sound velocity profile varying with depth, a short description of this method is presented. It has been shown [4] that the reflection of plane waves on an elastic half-space is equivalent to total reflection ($|R(\lambda_n| = 1$) on an interface at a

pseudo-depth $D + \Delta D(\lambda_n)$ where $\Delta D(\lambda_n)$ is, in general, complex (figure 3.1). It has also been shown [3] that solving (3.12) is equivalent to solving

$$\begin{aligned} & \gamma_n(1 + e^{i2\gamma_n D} R(\lambda_n)) = 0 \\ \Leftrightarrow\ & 1 + e^{i2\gamma_n D} R(\lambda_n) = 0 \end{aligned} \tag{3.13}$$

With this information in hand we can proceed to introducing the complex effective depth approach. Let $\Psi(\lambda_n)$ be the complex phase of the reflection coefficient defined

$$\Psi(\lambda_n) = -iR(\lambda_n) \tag{3.14}$$

Note that eq.(3.13) is equivalent to

$$R(\lambda_n) e^{i2\gamma_n D} = e^{i(2n\pi - \pi)} \tag{3.15}$$

and if we apply ln(.) in the above equation and multiply by $-i$ we get

$$\Psi(\lambda_n) + 2\gamma_n D - 1 = 2(n-1)\pi \tag{3.16}$$

Since the shift $\Delta D(\lambda_n)$ is defined as [4]

$$\Delta D(\lambda_n) = \frac{\Psi(\lambda_n) + \pi}{2\gamma_n} \tag{3.17}$$

we can substitute (3.16) into (3.17) and solve for γ_n, thus we have

$$\gamma_n = \frac{n\pi}{D + \Delta D(\lambda_n)} \tag{3.18}$$

Eventually the effective depth method can be implented to compute the $n-th$ eigenvalue of the depth problem iteratively as follows [6]: For some initial value λ_n^0 of λ_n

1. $for\ j = 1, 2, \ldots$
2. $\Delta D_j(\lambda_n^{j-1}) = \frac{\Psi(\lambda_n^{j-1}) + \pi}{2\gamma_n^{j-1}}$
3. $\gamma_n^j = \frac{n\pi}{D + \Delta D_j(\lambda_n^{j-1})}$
4. $\lambda_n^j = \sqrt{k^2 - {\gamma_n^j}^2}$

where the superscript j is refered to as the index of iteration. In addition, the initial value λ_n^0 corresponds to a low grazing angle, e.g. $\theta = 0.01$.

Thus, for $n = 1, 2, 3, \ldots$ one obtains the eigenvalues of the problem (3.4),(3.2),(3.3). The solution is completed with the computation of the coefficients A_n in (3.8) for the eigenfunctions u_n, using the normalization condition as proposed by Bucker [1] and Westwood *et al.* [5]. That is

$$\int_0^D u_n^2(z)dz - \frac{1}{2\lambda_n} \cdot \frac{d}{d\lambda}\left(\frac{1}{I(\lambda)}\right)\Big|_{\lambda=\lambda_n} \cdot u_n^2(D) = 1 \tag{3.19}$$

where the integral can be computed either analytically or numerically using the trapezoidal rule and the derivative of the inverse of the impedance function is well approximated using a finite difference scheme or can be expressed exactly after differentiation. It is noted that a detailed description of the derivation of the normalization constant is included in appendix A.

3.2. Sound speed profile varying with depth

If the sound velocity is varying with depth, then the wavenumber $k(z)$ is varying, as well as the vertical component of the wavenumber defined now as $\gamma_n(z) = \sqrt{k^2(z) - \lambda_n^2}$. Consequently there is no analytic solution for the differential equation of the depth problem (3.4),(3.2),(3.3) thus, it has to be solved numerically. The numerical method used in this work is the finite difference approximation.

Before getting into details it is noted that a varying velocity profile does not affect the expression for the impedance function (3.10) since without loss of generality it can be assumed that in an infinitesimally small interval $[D - \varepsilon, D]$ the sound speed remains constant. Thus, in this interval, the expression of the solution for eq.(3.4) is in the form (3.9) which leads to the same expression for the impedance function.

Our purpose is to pose the discrete analogue problem to (3.4),(3.2),(3.3) and formulate it as a matrix eigenvalue problem. Thus, we devide the interval $[0, D]$ into N intervals of length h, that is $N + 1$ points such that

$$z_j = jh \tag{3.20}$$

$$u_n(z_j) = u_n^j \ , \ u_n^0 = 0 \tag{3.21}$$

$$k(z_j) = k_j \ , \ j = 0, 1, 2, \ldots, N \tag{3.22}$$

and approximate $\frac{d^2 u_n^j}{dz^2}$ using the centred finite difference formula

$$\frac{d^2 u_n^j}{dz^2} \approx \frac{u_n^{j-1} - 2u_n^j + u_n^{j+1}}{h^2} \ , \ j = 1, 2, \ldots, N-1 \tag{3.23}$$

Substituting this approximation to the differential equation (3.4) and using (3.20)-(3.22) we get

$$\begin{aligned} &\frac{u_n^{j-1} - 2u_n^j + u_n^{j+1}}{h^2} + (k_j^2 - \lambda_n^2) u_n^j = 0 \ , \ j = 1, 2, \ldots, N-1 \\ \Leftrightarrow \ & u_n^{j-1} + (h^2 k_j^2 - 2) u_n^j + u_n^{j+1} = h^2 \lambda_n^2 u_n^j \end{aligned} \tag{3.24}$$

where the expression (3.24) indicates a linear system of $N - 1$ equations with N unknowns. These unknowns are the discrete values $u_n^j \ , \ j = 1, 2, \ldots, N$ of the eigenfunction $u_n(z)$. Note that the value $u_n^0 = u_n(0)$ is always known and equal to zero. For a well posed linear system an additional equation is needed and is derived below.

We expand in Taylor series the eigenfunction u_n about depth D and ignore terms of third order and beyond, thus we set

$$u_n(z) = u_n(D) + (z-D)u'_n(D) + (z-D)^2\frac{u''_n(D)}{2}$$

$$(z = D-h) \Rightarrow u_n(D-h) = u_n(D) - hu'_n(D) + h^2\frac{u''_n(D)}{2}$$

$$(3.4) \Rightarrow u_n(D-h) = u_n(D) - hu'_n(D) - h^2\frac{(k^2(D)-\lambda_n^2)u_n(D)}{2} \tag{3.25}$$

where the primes imply differentiation with respect to depth z. Eq.(3.3) can be written as $u'_n(D) = \frac{u_n(D)}{I(\lambda_n)}$ and substituting this expression into (3.25), after factorization we obtain

$$2u_n(D-h) + \left[h^2k^2(D) - 2 + \frac{2h}{I(\lambda_n)}\right]u_n(D) = h^2\lambda_n^2 u_n(D)$$

which according to (3.20)-(3.22) is equivalent to

$$2u_n^{N-1} + \left[h^2k_N^2 - 2 + \frac{2h}{I(\lambda_n)}\right]u_n^N = h^2\lambda_n^2 u_n^N \tag{3.26}$$

Now expressions (3.24) and (3.26) form a well posed $N \times N$ linear system of equations with unknowns the discrete values u_n^j , $j = 1, 2, \ldots, N$. This system is expressed in matrix form as

$$\frac{1}{h^2}\begin{bmatrix} h^2k_1^2-2 & 1 & 0 & \ldots & 0 \\ 1 & h^2k_2^2-2 & 1 & \ldots & 0 \\ \vdots & & \ddots & & \vdots \\ 0 & \ldots & 1 & h^2k_{N-1}^2-2 & 1 \\ 0 & 0 & \ldots & 2 & h^2k_N^2-2+\frac{2h}{I(\lambda_n)} \end{bmatrix}\begin{bmatrix} u_n^1 \\ u_n^2 \\ \vdots \\ u_n^{N-1} \\ u_n^N \end{bmatrix} = \lambda_n^2\begin{bmatrix} u_n^1 \\ u_n^2 \\ \vdots \\ u_n^{N-1} \\ u_n^N \end{bmatrix} \tag{3.27}$$

where the $N\times N$ matrix is denoted by $A(\lambda_n)$ and is a tridiagonal complex matrix depending on λ_n through the impedance function. That is, the depth problem (3.4),(3.2),(3.3) is reduced to a matrix eigenvalue problem and for a non-trivial solution λ_n must satisfy

$$det\left(A(\lambda_n) - \lambda_n^2 I\right) = 0 \tag{3.28}$$

where I indicates the identity matrix. An iterative technique based on Inverse Power Iteration method is presented in chapter 4 for estimating these λ_n. Given the eigenvalues, u_n^j can be computed by setting an arbitrary value for u_n^N and using backward computation, that is

$$u_n^N = 1 \tag{3.29}$$

$$u_n^{N-1} = \frac{1}{2}\left(h^2\lambda_n^2 - h^2k_N^2 + 2 - \frac{2h}{I(\lambda_n)}\right)u_n^N \tag{3.30}$$

$$u_n^j = \left(h^2\lambda_n^2h^2k_{j+1}^2 - 2\right)u_n^{j+1} - u_n^{j+2} \ , \ j = N-2, \ldots, 2, 1 \tag{3.31}$$

Note that setting an arbitrary value for u_n^N is permissable since if $\mathbf{u_n}$ satisfies an eigenvalue problem then so does $c\mathbf{u_n}$ with $c = constant$. Thus $\mathbf{u_n}$ can always be scaled so that $u_n^N = 1$. In practice, after backward computation a normalization condition as in (3.19) is applied. Now the integral term can be computed only by means of numerical integration (e.g. the trapezoidal rule). Eventually discrete values of the eigenfunctions are obtained and the computation of the pressure field is possible.

In this chapter the depth problem was defined and two cases were studied. These are the case of constant enviromental parameters and the case of a varying sound velocity. The influence of the seabed on the acoustic field in the water column was provided by an appropriate impedance function which was constructed. In the first case analytic expression for the eigenfunctions where used whereas in the second case the finite difference approximation was implemented and lead to a linear system of equations. In the case of a varying with depth sound speed profile the method for estimating the eigenvalues has not been presented in this chapter since it is described in details in chapter 4.

4. Estimation of eigenvalues for a sound velocity profile varying with depth

In this chapter an alternative method for the calculation of the complex eigenvalues of the depth problem is presented. Since in the case of a constant sound speed profile the method for estimating the eigenvalues has been presented in section 3.1, the following technnique concerns the case of a sound speed profile varying with depth.

It has been shown (section 3.2) that a finite difference approach for the depth problem in the varying velocity case, leads to a matrix eigenvalue problem (3.27) which is not a typical one since the matrix depends on the eigenvalue ($A = A(\lambda_n)$). An iterative procedure based on Inverse Power Iteration is presented for the estimation of the eigenvalues. The starting eigenvalues are those of a constant sound speed profile and are obtained using the Effective Depth method (section 3.1). Before getting into details for the iterative scheme a short description of the Inverse Power Iteration is given.

4.1. Inverse Power Iteration

Inverse Power Iteration method is a special case of the Power method, so the latter is presented first. Both methods are iterative and are used to approximate eigenvalues and eigenvectors [7].

Let $A \in \mathbb{C}^{\mathbb{N}\times\mathbb{N}}$ be a constant and diagonalizable matrix, $X^{-1}AX = diag[\lambda_1, \lambda_2, \ldots, \lambda_N]$, $X = [x_1, x_2, \ldots, x_N]$ and $|\lambda_1| > |\lambda_2| >, \ldots, > |\lambda_N|$. If v^0, $||v^0||_2 = 1$ then the sequence of vectors $\{v^k\}_k$ produced by

1. for $k = 1, 2, \ldots$
2. $\quad y^k = Av^{k-1}$
3. $\quad v^k = y^k/||y^k||_2$

converges to a vector v. This vector is an eigenvector of A associated with the eigenvalue λ_1 which can be computed by

$$\lambda_1 = \frac{v^H A v}{v^H v}$$

where the superscript H indicates the conjugate transpose. That is the Power method approximates the eigenvector corresponding to the dominant eigenvalue. In order to approximate eigenvectors associated with eigenvalues $\lambda_2, \lambda_3, \ldots, \lambda_N$ the idea of Power

method is extended and forms Inverse Power Iteration usually refered to as Inverse Iteration. That is,

Let A be a constant matrix and μ an approximation to λ where λ is an eigenvalue of A. If v^0, $||v^0||_2 = 1$ then the sequence of vectors $\{v^k\}_k$ produced by

1. for $k = 1, 2, \ldots$
2. *solve* $(A - \mu I)y^k = v^{k-1}$
3. $v^k = y^k / ||y^k||_2$

converges to a vector v. This vector is an eigenvector of A associated with the closest eigenvalue to μ and is calculated by formula

$$\lambda = \mu + \frac{v^H A v}{v^H v}$$

Note that Inverse Iteration is the same as Power method with matrix A replaced by $(A - \mu I)^{-1}$. Also note that $(A - \mu I)$ is invertible since μ is an approximation to an eigenvalue.

4.2. Calculation of the eigenvalues by means of an iterative scheme

With this information in hand one could suppose that provided some initial assumptions, the complex eigenvalues of problem (3.27) can be determined using Inverse Iteration. The problem is that in our case the finite difference matrix depends on the eigenvalue ($A = A(\lambda_n)$). The main idea to overcome this problem is that Inverse Iteration be used *iteratively*. That is, after having obtained an approximation λ_n^1 by Inverse Power Iteration, to compute a new finite difference matrix $A(\lambda_n^1)$ on which Inverse Iteration is applied again and then continue consecutively until the sequence $\{\lambda_n^i\}_i$ converges.

A representation of the idea described above in brief is :

1. initial assumption λ_n^0
2. apply Inverse Iteration to $A(\lambda_n^0)$ with $\mu = \lambda_n^0$ to obtain λ_n^1
3. apply Inverse Iteration to $A(\lambda_n^1)$ with $\mu = \lambda_n^1$ to obtain λ_n^2

   $\vdots$

   continue

   $\vdots$

Based on this idea an iterative technique was developed. As initial approximations of the eigenvalues, we have chosen to use the eigenvalues of a constant sound speed profile close to the actual one, using the effective-depth method. Thus, the suggested iterative scheme is as follows :

1. $\mu_n = effectiveDepth\,(c_0, [ENV])\ ,\ c_0 = const.$
2. $\lambda_n^0 \leftarrow \mu_n$
3. $until\ \{\lambda_n^i\}_i\ converges$
4. $\lambda_n^{i+1} = InvPowIt\left(\lambda_n^i, A(\lambda_n^i)\right)\ ,\ i = 0, 1, 2, \ldots$

where the bracket $[ENV]$ implies the environmental parameters.

Having studied the application of the above scheme in waveguides with different sound speed profiles and environmental parameters, several issues have to be stressed out :

- We apply the Effective Depth scheme for the initial assumption of the eigenvalues with $c_0 = min_{z\in[0,D]}\{c(z)\}$. This choice guarantees computation of low order modes which otherwise could be omitted.
- The suggested scheme may generate duplicates due to the fact that some of the initial assumptions $\lambda_n^0\ ,\ n = 1, 2, 3, \ldots$ may be close to each other enough and the iteration leads to the same limit. It is obvious that these duplicates should be excluded from the computation of the pressure field
- It is still possible that the iterative scheme omits some eigenvalues. We overcome this by applying a high to low reordering of eigenvalues according to their real part and taking the mean value between two adjacent eigenvalues. This value is then used as an initial approximation to the suggested iterative scheme

Note that the third issue mentioned above can be applied more than once making the eigenvalue search more extended. It can also be applied right after having obtained the initial assumptions by the effective depth yielding more initial approximations. One could also notice that although the method of Inverse Iteration also provides approximations to the eigenvectors, that is discrete values of the eigenfunctions, we choose to calculate these values as described in section 3.2. This choice is made in order not to save in memory the unwanted duplicates mentioned above, since it is not known *a priori* how many of them will be generated.

5. Applications - Results

In order to illustrate the effiency of the technique described in chapters 3 and 4, the eigenvalues and discrete values of the associated eigenfunctions of the depth problem are approximated for several cases. Results for all interesting measures concerning the acoustic pressure field are compared to those produced by the KRAKEN-C Normal Mode Program. These measures are the eigenvalues, the eigenfunctions and the transmission loss which is calculated at the source depth. Results for both constant and varying velocity profiles are included. In the case of a constant profile the effective depth method is implemented for the computation of the eigenvalues, however the eigenfunctions are obtained by use of the finite difference approach. In cases that the propagated modes are too many, only a number of the principal ones will be presented.

5.1. Constant sound speed profile

In the first place the efficiency of the effective depth approach is presented. Thus, a waveguide of constant sound velocity is considered, set at $c(z) = 1500\ m/sec$. The depth of the waveguide is 400 m and the velocities of compressional and shear waves in the seabed are $c_2 = 1700\ m/sec$ and $c_s = 500\ m/sec$ respectively, whereas the density in the water is $\rho = 1000\ kg/m^3$ and $\rho_2 = 1300\ kg/m^3$ in the seabed. A monochromatic point source is located at depth $z_0 = 360\ m$ and the following results concern two different cases of its frequency, when $f = 20\ Hz$ and $f = 40\ Hz$.

5.1.1. When the source frequency is $20\ Hz$

In table 5.1 the eigenvalues concerning an environment of constant sound speed profile are presented as computed by the effective depth method and by KRAKEN-C. It is obvious that the eigenvalues obtained by both these approaches coincide. The first ten associated eigenfunctions are shown in figures 5.1 and 5.2 indicating the real and imaginary parts respectively. The thick black line corresponds to results produced by KRAKEN-C and the thiner green line to the technique described in a previous chapter.

The measurements for the corresponding transmission loss is presented in figure 5.3 where it is shown that the eigenvalues obtained by the effective depth lead to a good approximation of the pressure field. Transmission loss was calculated along a 5 km range in the horizontal direction at the source depth.

Mode	Effective Depth	KRAKEN-C
1	8.34416433e-02 + i3.34528906e-06	8.34416441e-02 + i3.34525416e-06
2	8.24372080e-02 + i1.20962221e-05	8.24372209e-02 + i1.20957776e-05
3	8.07581679e-02 + i2.20201778e-05	8.07582328e-02 + i2.20187524e-05
4	7.84055138e-02 + i2.52802636e-05	7.84057182e-02 + i2.52789938e-05
5	7.54330315e-02 + i1.20070710e-05	7.54335150e-02 + i1.20102943e-05
6	7.18927897e-02 + i6.93543927e-04	7.18940917e-02 + i6.93321721e-04
7	6.65430214e-02 + i1.42525034e-03	6.65458029e-02 + i1.42505717e-03
8	5.96862684e-02 + i2.10647742e-03	5.96917522e-02 + i2.10630781e-03
9	5.07460587e-02 + i2.90121252e-03	5.07566119e-02 + i2.90088216e-03
10	3.83550534e-02 + i4.22135860e-03	3.83765611e-02 + i4.21964878e-03
11	1.76713446e-02 + i9.72793015e-03	1.77259197e-02 + i9.69991435e-03

Table 5.1.: The eigenvalues as computed with the Effective Depth and with KRAKEN-C for test case 5.1.1

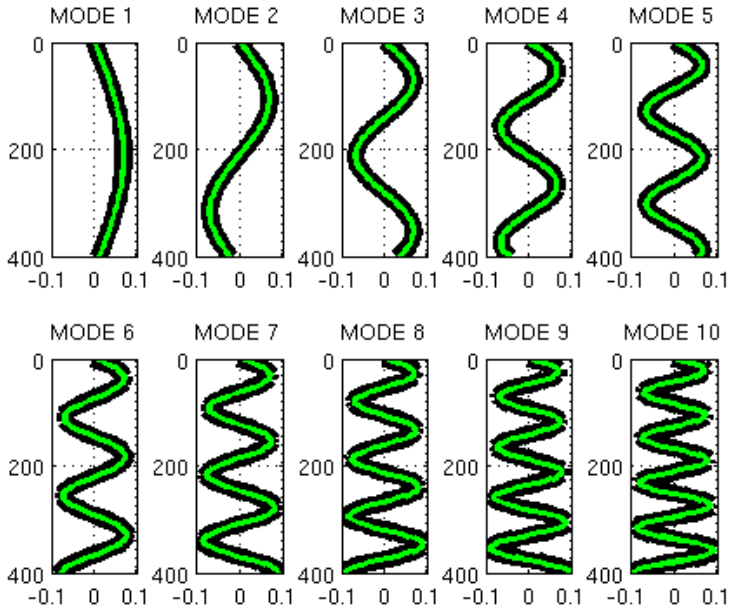

Figure 5.1.: Real part of the first ten eigenfunctions for test case 5.1.1

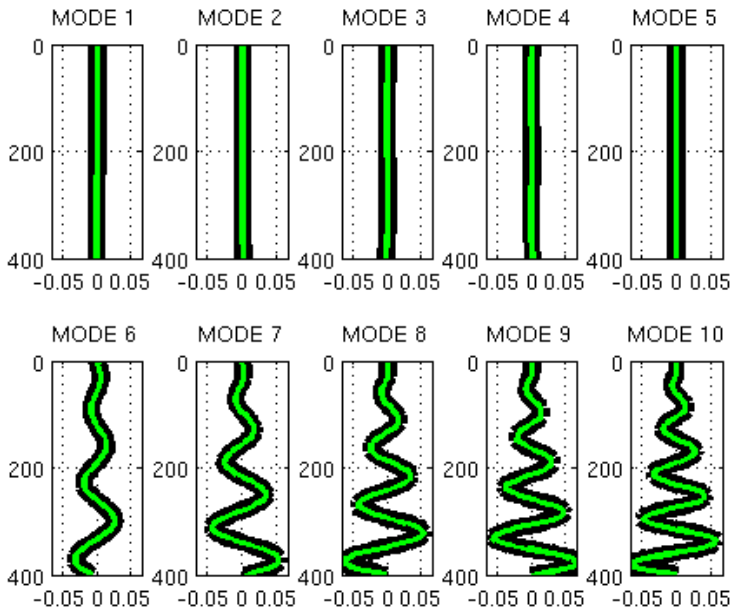

Figure 5.2.: Imaginary part of the first ten eigenfunctions for test case 5.1.1

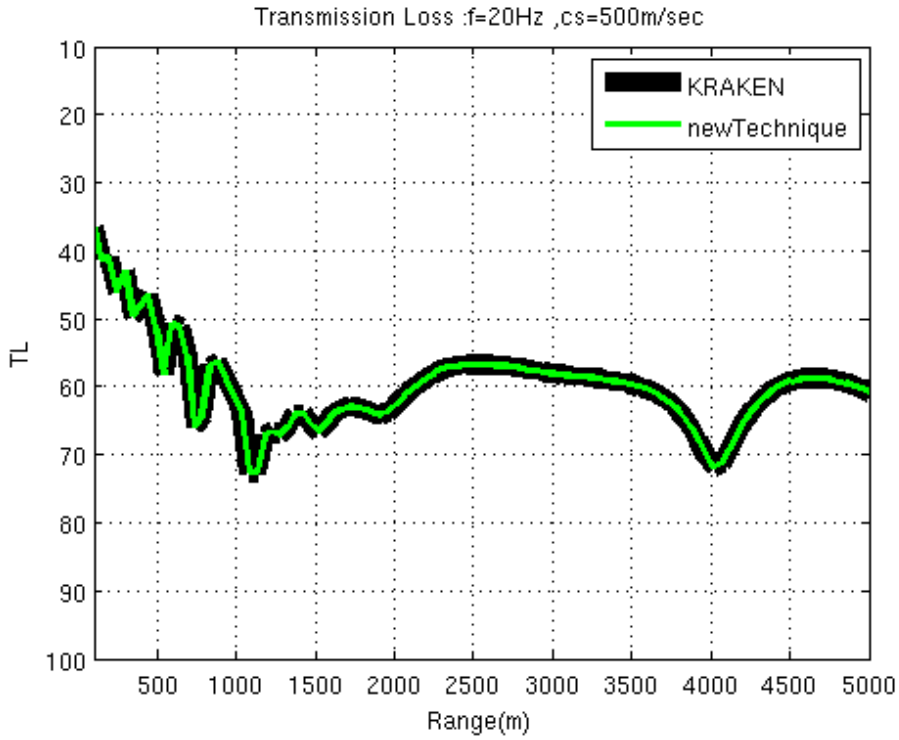

Figure 5.3.: Transmission loss calculated at the source depth $z_0 = 360\ m$ for test case 5.1.1

5.1.2. When the source frequency is 40 Hz

For a more integrated testing of the efficiency of the effective depth approach, measurements for a higher source frequency of 40 Hz are also included. In table 5.2 the first ten eigenvalues of the depth problem, as computed by the effective depth and KRAKEN-C are presented. The real and imaginary part of the associated eigenfunctions are shown in figures 5.4 and 5.5 respectively while the comparison for the transmission loss is presented in figure 5.6. The black thick line corresponds to KRAKEN-C and the green line to computations based on eigenvalues obtained with the effective depth method. It is obvious that both techniques yield coinciding results.

Mode	Effective Depth	KRAKEN-C
1	1.67376324e-01 + i9.19665756e-07	1.67376325e-01 + i9.19655009e-07
2	1.66849787e-01 + i3.59678864e-06	1.66849795e-01 + i3.59662391e-06
3	1.65969949e-01 + i7.77643452e-06	1.65969989e-01 + i7.77566455e-06
4	1.64733435e-01 + i1.30033622e-05	1.64733563e-01 + i1.30012125e-05
5	1.63135640e-01 + i1.85799558e-05	1.63135952e-01 + i1.85756080e-05
6	1.61170950e-01 + i2.35184625e-05	1.61171601e-01 + i2.35117089e-05
7	1.58833340e-01 + i2.65094193e-05	1.58834553e-01 + i2.65016740e-05
8	1.56118080e-01 + i2.59521954e-05	1.56120163e-01 + i2.59474833e-05
9	1.53027714e-01 + i2.01396657e-05	1.53031064e-01 + i2.01447099e-05
10	1.49605594e-01 + i7.88388026e-06	1.49610577e-01 + i7.90487556e-06

Table 5.2.: The first ten eigenvalues as computed with the Effective Depth and with KRAKEN-C for test case 5.1.2

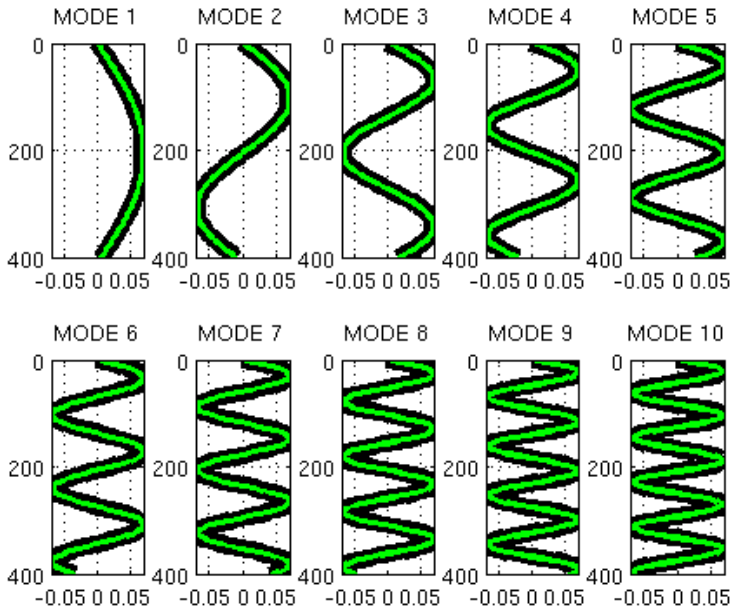

Figure 5.4.: Real part of the first ten eigenfunctions for test case 5.1.2

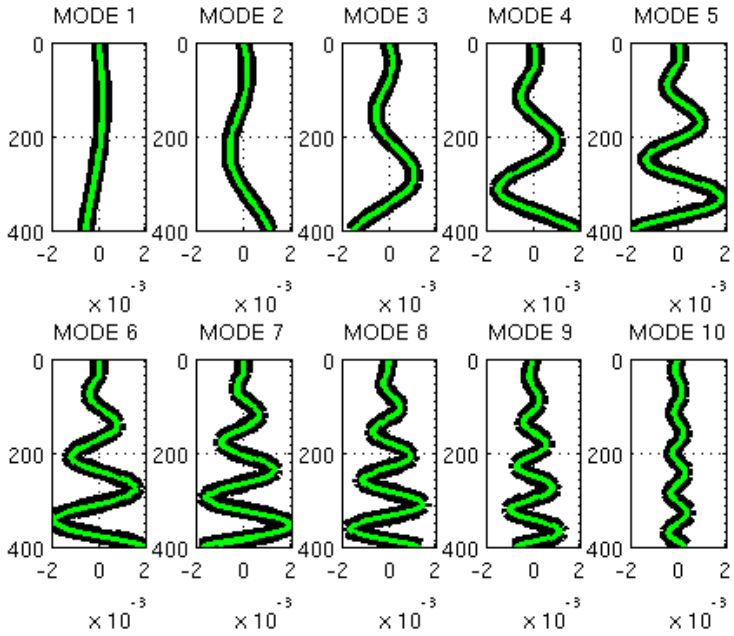

Figure 5.5.: Imaginary part of the first ten eigenfunctions for test case 5.1.2

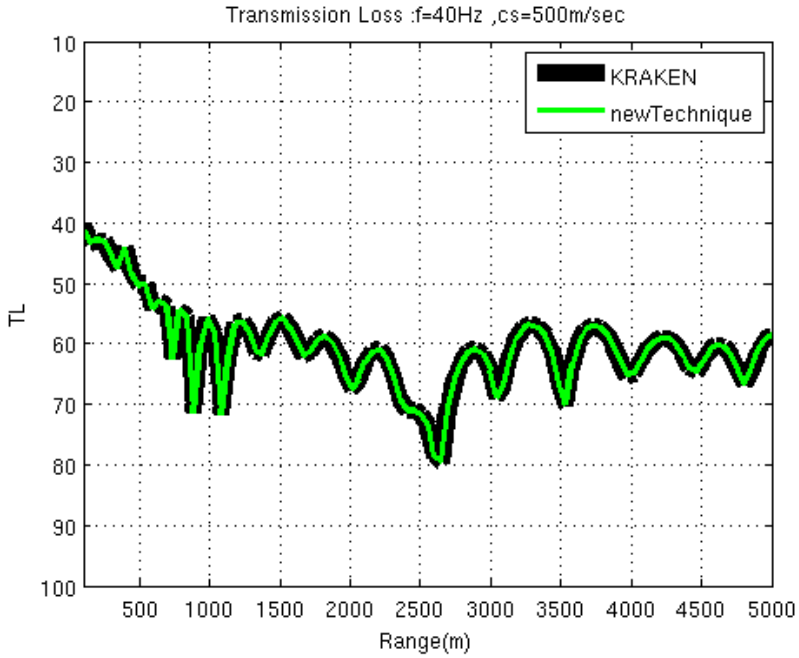

Figure 5.6.: Transmission loss calculated at the source depth $z_0 = 360\ m$ for test case 5.1.2

5.2. Sound speed profile varying with depth

Having tested the efficiency of the effective depth method for the computation of the eigenvalues of the depth problem with a constant sound velocity profile, we proceed with presenting the efficiency of the technique suggested in chapter 4 for the estimation of the eigenvalues in environments with a sound speed profile varying with depth.

Several test cases have been studied for various environmental parameters including different waveguide depths, shear wave speeds in the bottom, sound speed profiles in the water and of course the cases tested concern various source frequencies. The environmental parameters which are common for all test cases are the densities in the water and the seabed set at $\rho = 1000\ kg/m^3$ and $\rho_2 = 1300\ kg/m^3$ respectively and the velocity of compressional waves in the seabed set at $c_2 = 1700\ m/sec$.

5.2.1. Linearly increasing sound speed over a soft elastic bottom

In this test case a 500 m deep waveguide is considered and the velocity of shear waves in the bottom is $c_s = 200\ m/sec$. The sound speed profile is shown in table 5.3 which implies linear interpolation between the given values. A monochromatic point source is located at depth $z_0 = 400\ m$ and emits in frequency $f = 20\ Hz$. In table 5.4, the

$z\ (m)$	$c(z)\ (m/sec)$
0	1490
500	1550

Table 5.3.: The sound speed profile for the test case of subsection 5.2.1

eigenvalues as computed by the suggested iterative technique and by KRAKEN-C are presented. One can see that results produced by the two programs coincide. As in the constant sound speed case, the first ten eigenfunctions are presented in figures 5.7 and 5.8. The former corresponds to the real part of the eigenfunctions and the latter to the imaginary part. Last, in figure 5.9 a comparison of the transmission loss along a 5 km range is shown. As previously the black line refers to results produced by KRAKEN-C and the green line to our results.

Note that in figure 5.8, the imaginary part of modes 1-6 is practically zero (10^{-6}) while modes of higher order are given some rise. This is normal since the imaginary part of a mode is related to the absorption of acoustic energy and as it is known low order modes have a greater contribution to the acoustic field than the ones of higher order. As shown in figures 5.7-5.9 the two programs coincide in the calculation of both the eigenfunctions and the transmission loss.

Mode	new technique	KRAKEN-C
1	8.28284167e-02 + i8.16865720e-10	8.28284167e-02 + i8.16865720e-10
2	8.16929949e-02 + i6.36670471e-08	8.16929948e-02 + i6.36669669e-08
3	8.05798842e-02 + i4.04607133e-07	8.05798842e-02 + i4.04606672e-07
4	7.91141190e-02 + i7.51998431e-07	7.91141188e-02 + i7.52000104e-07
5	7.71838721e-02 + i7.27565344e-07	7.71838816e-02 + i7.27438872e-07
6	7.48125809e-02 + i2.45105588e-07	7.48129193e-02 + i2.40958374e-07
7	7.19176653e-02 + i4.42424216e-04	7.19173049e-02 + i4.42287613e-04
8	6.79771774e-02 + i8.16790905e-04	6.79771960e-02 + i8.16591254e-04
9	6.31712898e-02 + i1.18282953e-03	6.31713408e-02 + i1.18238626e-03
10	5.72856763e-02 + i1.60233840e-03	5.72856462e-02 + i1.60227786e-03
11	4.99457086e-02 + i2.15131729e-03	4.99457280e-02 + i2.15127892e-03
12	4.03862396e-02 + i3.01971321e-03	4.03862666e-02 + i3.01969738e-03
13	2.64816812e-02 + i5.11551485e-03	2.64816592e-02 + i5.11551248e-03

Table 5.4.: The eigenvalues computed with the suggested technique and with KRAKEN-C for test case 5.2.1

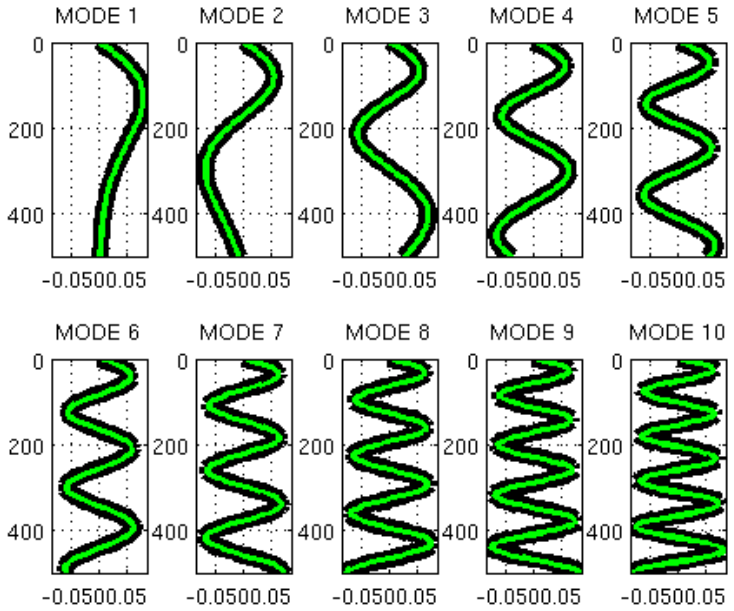

Figure 5.7.: Real part of the first ten eigenfunctions for test case 5.2.1

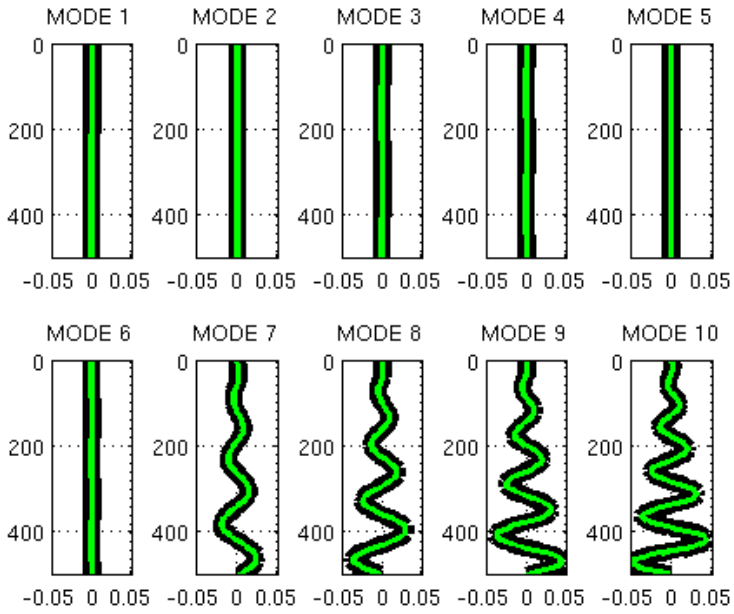

Figure 5.8.: Imaginary part of the first ten eigenfunctions for test case 5.2.1

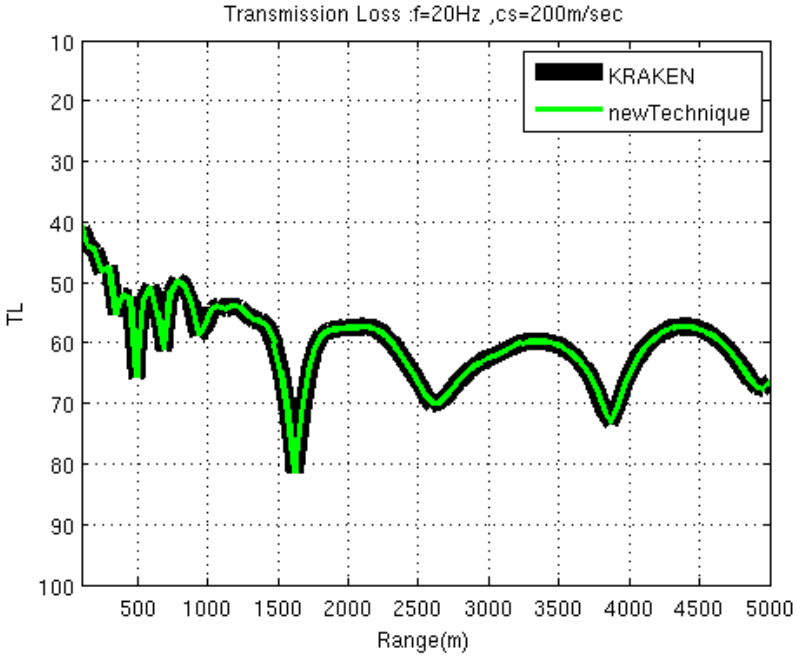

Figure 5.9.: Transmission loss calculated for test case 5.2.1

5.2.2. Linearly increasing sound speed over a hard elastic bottom

This test case is similar to case 5.2.1 with the difference that the waveguide is of depth 800 m and the velocity of shear waves in the bottom is set at $c_s = 500\ m/sec$, that is a harder seabed than previously. The source is located at depth $z_0 = 560\ m$ and the sound speed profile is assumed similar to that of the previous case as shown in table 5.5. Results for three different values of the source frequency are presented. It is noted that the black thick line refers to results as computed by KRAKEN-C whereas the green colour corresponds to results obtained by our method.

$z\ (m)$	$c(z)\ (m/sec)$
0	1490
800	1550

Table 5.5.: The sound speed profile for the test case of subsection 5.2.2

When the source frequency is 20 Hz

In such an environment the propagating modes are twenty one. The first ten of these, as calculated by the suggested technique are shown in table 5.6 in comparison to those computed by KRAKEN-C. The real and imaginary part of the associated eigenfunctions are presented in figures 5.10 and 5.11 while the transmission loss is illustrated in figure 5.12. Note that imaginary part of modes 1-9 is in practice null whereas mode 10 is the first to present a remarkable amplitude. It is obvious that results produced by the method suggested in this work coincide with those produced by KRAKEN-C.

Mode	new technique	KRAKEN-C
1	8.32329795e-02 + i8.03137318e-12	8.32329795e-02 + i8.03138015e-12
2	8.24116108e-02 + i5.16675533e-09	8.24116108e-02 + i5.16675631e-09
3	8.17377829e-02 + i2.50989131e-07	8.17377829e-02 + i2.50989137e-07
4	8.10864382e-02 + i2.01920560e-06	8.10864382e-02 + i2.01920571e-06
5	8.03147602e-02 + i5.41423370e-06	8.03147601e-02 + i5.41423592e-06
6	7.93545812e-02 + i8.68231210e-06	7.93546005e-02 + i8.68056234e-06
7	7.81998717e-02 + i1.06296775e-05	7.81998720e-02 + i1.06295185e-05
8	7.68551776e-02 + i1.02141437e-05	7.68553425e-02 + i1.01983692e-05
9	7.53357296e-02 + i6.30198206e-06	7.53356914e-02 + i6.30590139e-06
10	7.37975299e-02 + i9.26801678e-05	7.37990339e-02 + i9.46870023e-05

Table 5.6.: The first ten eigenvalues computed with the suggested technique and with KRAKEN-C for test case 5.2.2 with $f = 20\ Hz$

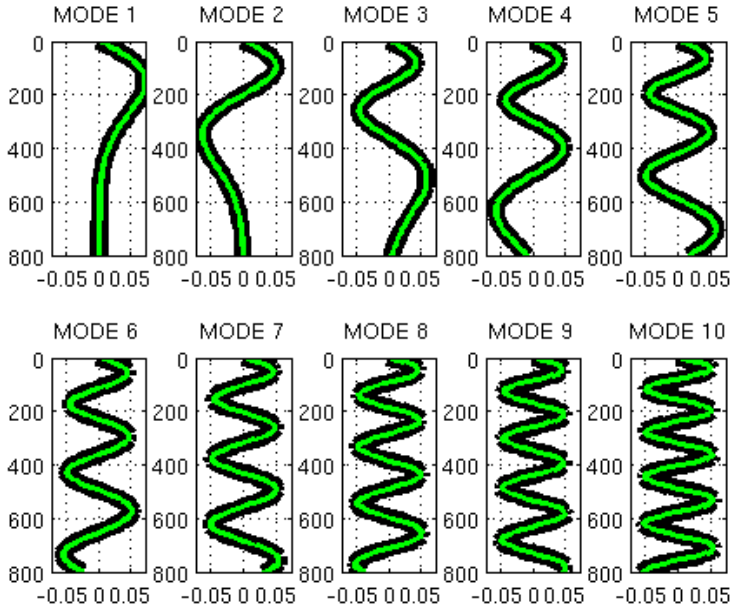

Figure 5.10.: Real part of the first ten eigenfunctions for test case 5.2.2 with $f = 20\ Hz$

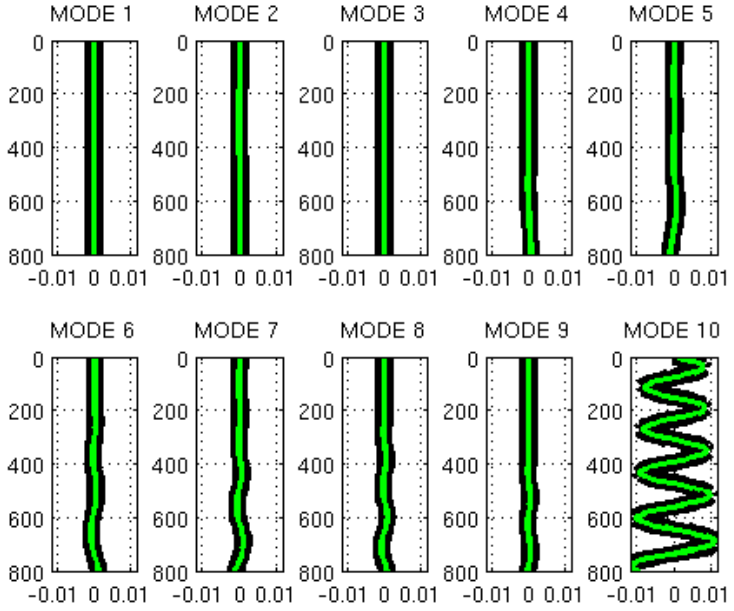

Figure 5.11.: Imaginary part of the first ten eigenfunctions for test case 5.2.2 with $f = 20\ Hz$

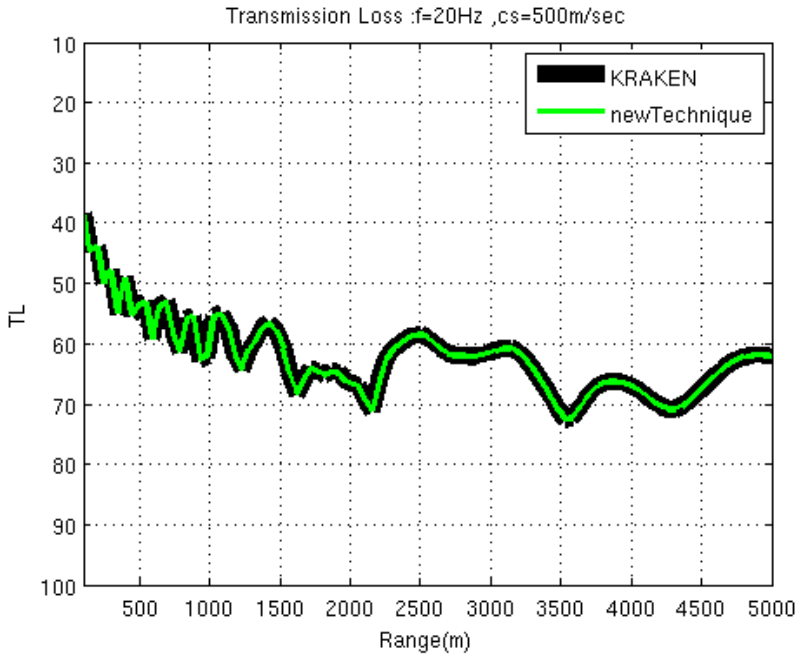

Figure 5.12.: Transmission loss calculated for test case 5.2.2 with $f = 20\ Hz$

When the source frequency is $50\ Hz$

Having encouraging results for a source of low frequency we have chosen to test our method also for higher values. Thus, all enviromental parameters are preserved whereas the source frequency is set at $50\ Hz$. For this value of frequency we also get results very close to these of KRAKEN-C's. Table 5.7 shows a comparison of the first ten eigenvalues as computed by our iterative scheme and KRAKEN-C. Figure 5.13 shows the real part of the first ten eigenfunctions whereas the figure with the corresponding imaginary part has been omitted since it is almost null. Last, in figure 5.14 the comparison for the transmission loss is presented.

Mode	new technique	KRAKEN-C
1	2.09342638e-01 + i4.96669270e-22	2.09342638e-01 + i-1.74630461e-19
2	2.08222436e-01 + i3.28976348e-21	2.08222436e-01 + i-2.72787198e-19
3	2.07308040e-01 + i1.06914108e-17	2.07308040e-01 + i1.07343685e-17
4	2.06501933e-01 + i7.19062751e-15	2.06501933e-01 + i7.19081766e-15
5	2.05766721e-01 + i1.55702680e-12	2.05766721e-01 + i1.55702766e-12
6	2.05083069e-01 + i1.32232616e-10	2.05083069e-01 + i1.32232616e-10
7	2.04439258e-01 + i4.84798755e-09	2.04439258e-01 + i4.84798755e-09
8	2.03825856e-01 + i7.77841897e-08	2.03825856e-01 + i7.77841900e-08
9	2.03223977e-01 + i5.33289840e-07	2.03223977e-01 + i5.33289778e-07
10	2.02590524e-01 + i1.71513141e-06	2.02590524e-01 + i1.71513158e-06

Table 5.7.: The first ten eigenvalues computed with the suggested technique and with KRAKEN-C for test case 5.2.2 with $f = 50\ Hz$

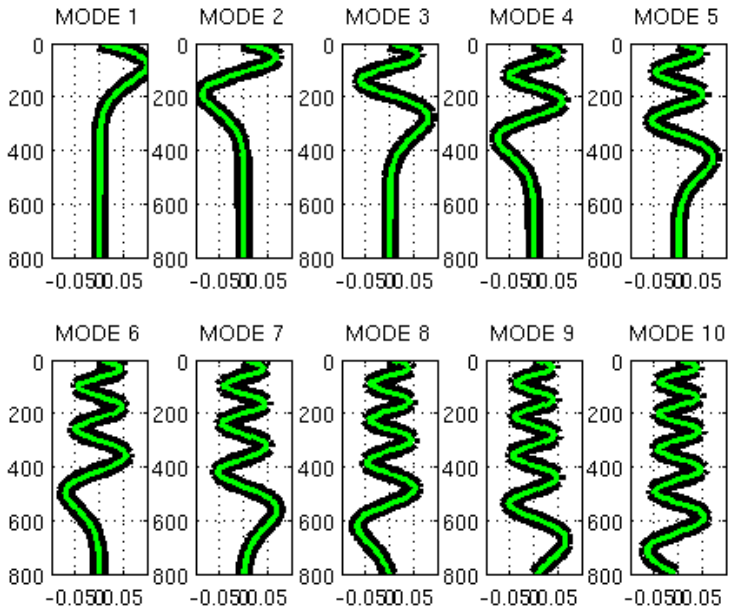

Figure 5.13.: Real part of the first ten eigenfunctions for test case 5.2.2 with $f = 50\ Hz$

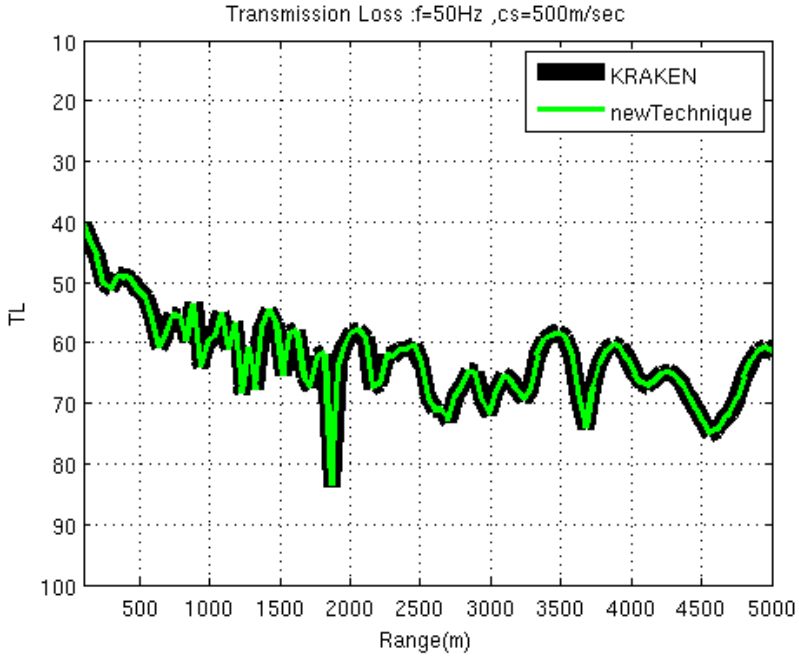

Figure 5.14.: Transmission loss calculated for test case 5.2.2 with $f = 50\ Hz$

When the source frequency is 80 Hz

The last subcase of the present test case studied, concerns an even higher source frequency. The frequency is now set at 80 Hz resulting in a greater number of propagating modes. The first ten, out of eighty five propagating, are presnted in table 5.8 and the real part of the corresponding eigenfunctions is shown in figure 5.15 whereas the imaginary part of these ten eigenfunctions is practically zero and is omitted. The transmission loss along a 5 km range is illustrated in figure 5.16. It is noted that for a higher value of frequency our scheme generates the desired results.

Mode	new technique	KRAKEN-C
1	3.35593916e-01 + i6.67567500e-23	3.35593916e-01 + i4.70836086e-19
2	3.34281716e-01 + i3.46836483e-28	3.34281716e-01 + i2.38907283e-19
3	3.33209779e-01 + i1.75774728e-27	3.33209779e-01 + i5.29641983e-19
4	3.32264172e-01 + i7.10040418e-27	3.32264172e-01 + i7.05521247e-20
5	3.31401222e-01 + i1.20229773e-23	3.31401222e-01 + i7.35653681e-19
6	3.30598357e-01 + i8.28293205e-21	3.30598357e-01 + i3.33723621e-19
7	3.29842005e-01 + i2.71925419e-18	3.29842005e-01 + i2.92573990e-18
8	3.29123203e-01 + i4.70545168e-16	3.29123203e-01 + i4.70689375e-16
9	3.28435644e-01 + i4.59326788e-14	3.28435644e-01 + i4.59341378e-14
10	3.27774674e-01 + i2.63901779e-12	3.27774674e-01 + i2.63901705e-12

Table 5.8.: The first ten eigenvalues computed with the suggested technique and with KRAKEN-C for test case 5.2.2 with $f = 80\ Hz$

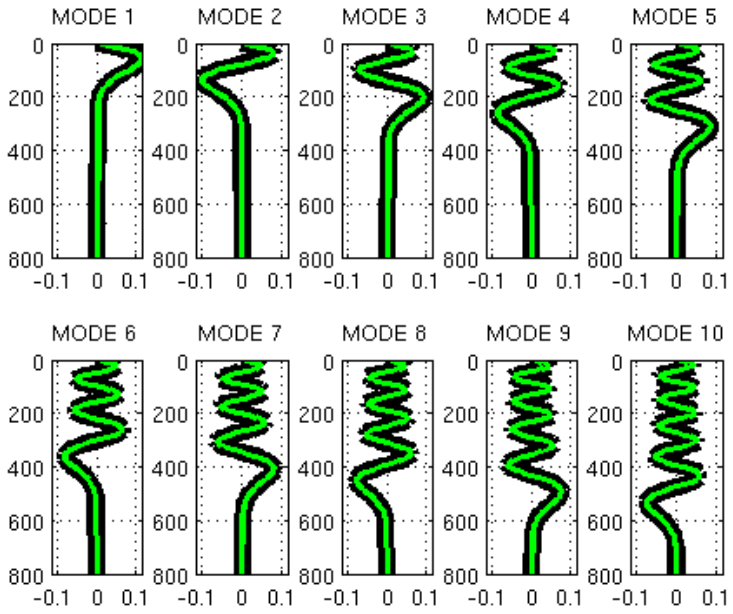

Figure 5.15.: Real part of the first ten eigenfunctions for test case 5.2.2 with $f = 80\ Hz$

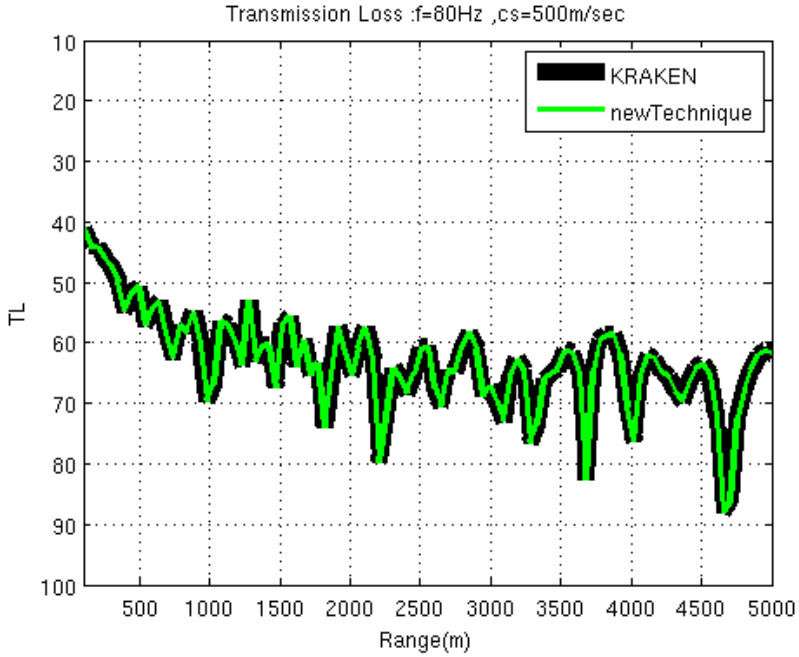

Figure 5.16.: Transmission loss calculated for test case 5.2.2 with $f = 80\ Hz$

5.2.3. Linearly varying sound speed with an alternating monotonicity

In this test case a more complex sound velocity profile is considered. We have chosen a profile which initially decreases linearly with depth and at some point the monotonicity changes and the sound speed increases linearly until the maximum depth is reached (table 5.9). The rest of the environmental parameters are considered as in test case 5.2.2, that is a waveguide of depth $D = 800\ m$, the densities of the two media are $\rho = 1000\ kg/m^3$ and $\rho_2 = 1300\ kg/m^3$ and the seabed is considered as a hard elastic half-space supporting a compressional wave velocity of $c_2 = 1700\ m/sec$ and a shear wave velocity of $c_s = 500\ m/sec$. For this case the technique suggested in chapter 4 for estimating the eigenvalues and the method of section 3.2 for the computation of the eigenfunctions are tested for three different values of source frequency, for $f = 20, 50, 80\ Hz$.

Last, the pressure field calculated in a whole rectangular domain and an extra test of the suggested algorithm for a 200 Hz source frequency are also presented, indicatively. It is noted that the black colour in the figures refers to results obtained by KRAKEN-C and the thin green line to results of our method.

$z\ (m)$	$c(z)\ (m/sec)$
0	1500
200	1490
800	1550

Table 5.9.: The sound speed profile for the test case of subsection 5.2.3

When the source frequency is 20 Hz

For a 20 Hz source frequency results and comparisons are shown in table 5.10 and figures 5.17 and 5.18. The table includes the first ten eigenvalues, out of twenty one propagating modes, using our technique and KRAKEN-C while figures 5.17 and 5.18 present a comparison between the two approaches for the real part of the eigenfunctions and the transmission loss of the acoustic pressure field. One concludes that the method described in this work provides results with accuracy.

Mode	new technique	KRAKEN-C
1	8.37800697e-02 + i4.89634681e-12	8.37800697e-02 + i4.89634533e-12
2	8.28821135e-02 + i1.97453303e-09	8.28821135e-02 + i1.97453305e-09
3	8.21318187e-02 + i1.04814827e-07	8.21318191e-02 + i1.04786014e-07
4	8.14230455e-02 + i1.22384275e-06	8.14230451e-02 + i1.22388877e-06
5	8.06400791e-02 + i4.40711188e-06	8.06400790e-02 + i4.40705172e-06
6	7.96835980e-02 + i8.12550757e-06	7.96836115e-02 + i8.12411915e-06
7	7.85324323e-02 + i1.06417449e-05	7.85324314e-02 + i1.06418614e-05
8	7.71924652e-02 + i1.08325297e-05	7.71924615e-02 + i1.08328739e-05
9	7.56738580e-02 + i7.61659835e-06	7.56738417e-02 + i7.61733769e-06
10	7.40553087e-02 + i1.55907081e-06	7.40540533e-02 + i5.94530072e-07

Table 5.10.: The first ten eigenvalues computed with the suggested technique and with KRAKEN-C for test case 5.2.3 with $f = 20\ Hz$

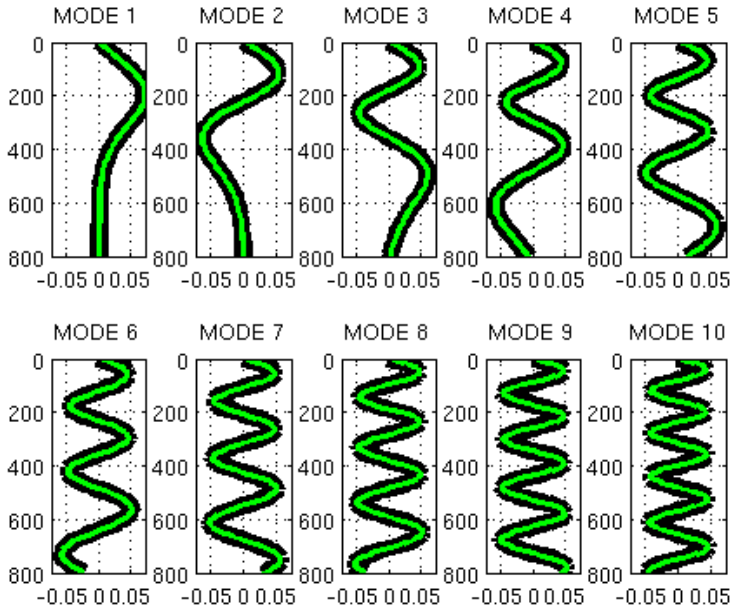

Figure 5.17.: Real part of the first ten eigenfunctions for test case 5.2.3 with $f = 20\ Hz$

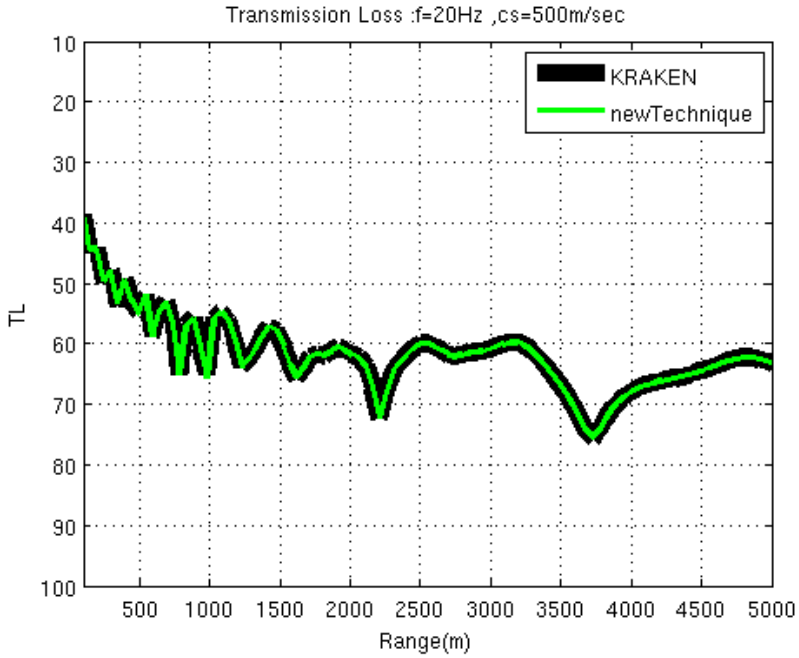

Figure 5.18.: Transmission loss calculated for test case 5.2.3 with $f = 20\ Hz$

When the source frequency is 50 Hz

We proceed with testing the same sound speed profile for a higher source frequency of 50 Hz. Results are still obtained with great accuracy. In table 5.11 the first ten eigenvalues, out of fifty three propagating modes, are shown as estimated by our method and by KRAKEN-C as well. Figures 5.19 and 5.20 present the real part of the associated eigenfunctions and the transmission loss along a 5 km range in the horizontal direction respectively.

Mode	new technique	KRAKEN-C
1	2.10223144e-01 + i6.21749319e-24	2.10223144e-01 + i-9.04229241e-19
2	2.09338118e-01 + i4.49041729e-21	2.09338118e-01 + i9.64913141e-19
3	2.08529674e-01 + i2.08728984e-18	2.08529674e-01 + i1.48127741e-18
4	2.07703700e-01 + i6.22953427e-16	2.07703700e-01 + i6.22751765e-16
5	2.06920705e-01 + i9.24544067e-14	2.06920705e-01 + i9.24546312e-14
6	2.06159864e-01 + i7.80467882e-12	2.06159864e-01 + i7.80467888e-12
7	2.05424360e-01 + i3.55851942e-10	2.05424360e-01 + i3.55851944e-10
8	2.04718315e-01 + i8.48157026e-09	2.04718315e-01 + i8.48157026e-09
9	2.04036830e-01 + i1.03191596e-07	2.04036830e-01 + i1.03191596e-07
10	2.03362097e-01 + i6.17017959e-07	2.03362097e-01 + i6.17017868e-07

Table 5.11.: The first ten eigenvalues computed with the suggested technique and with KRAKEN-C for test case 5.2.3 with $f = 50\ Hz$

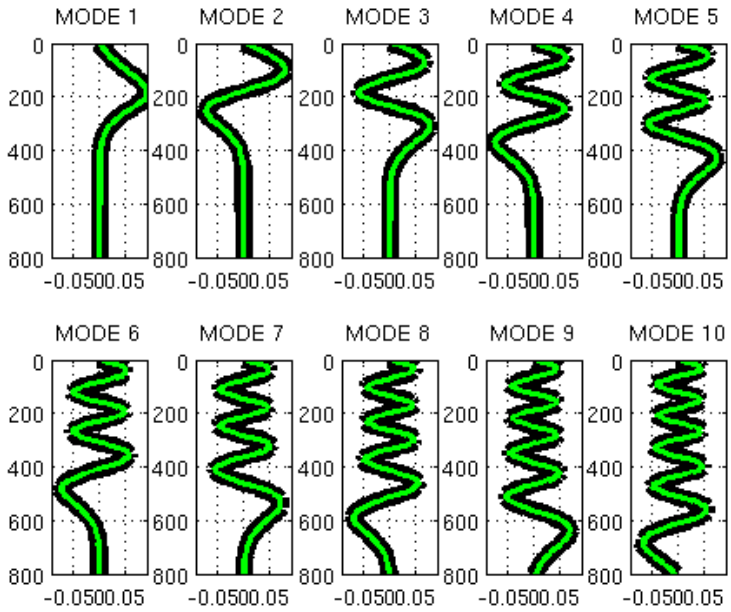

Figure 5.19.: Real part of the first ten eigenfunctions for test case 5.2.3 with $f = 50\ Hz$

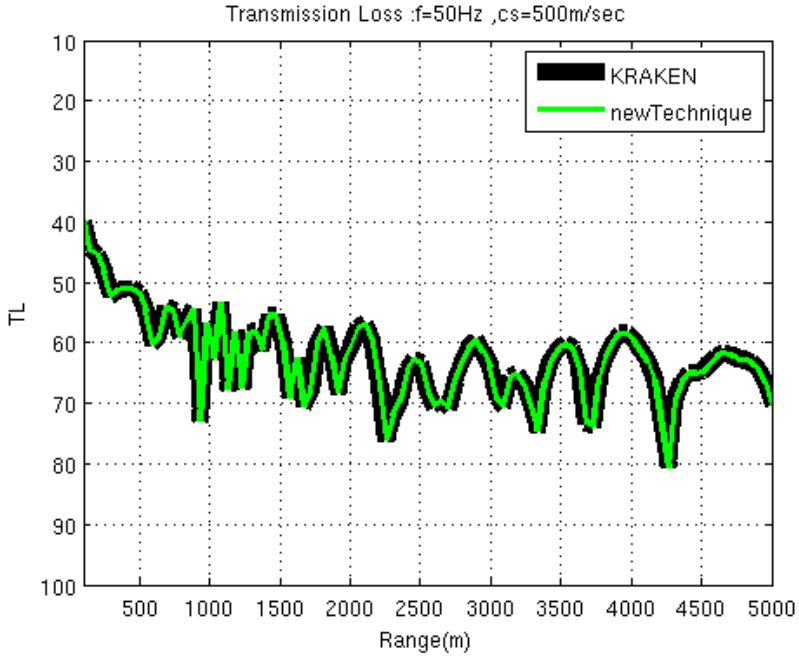

Figure 5.20.: Transmission loss calculated for test case 5.2.3 with $f = 50\ Hz$

When the source frequency is 80 Hz

In correspondence to test case 5.2.2 the scenario of an 80 Hz source frequency is included. Results generated by the suggested scheme are still satisfying according to KRAKEN-C. Table 5.12 shows the first ten eigenvalues and figures 5.21 and 5.22 correspond to the real part of the first ten eigenfunctions and the transmission loss respectively.

So far, the calculation of the transmission loss is presented for a specific depth z_0, that is the source depth. For completeness, in this case, both the pressure field and the transmission loss are presented as calculated in the whole rectangular domain $[0, r_{max}] \times [0, D]$ with $r_{max} = 5\ km$. Figure 5.23 represents the absolute value of the pressure field while figure 5.24 the corresponding transmission loss. The horizontal and vertical axes indicate the range and depth respectively, while the colour indicates the magnitude of the measurement. As expected, the acoustic field is appeared noticeably stronger close to the source location $(r_0, z_0) = (0, 560)$. Furthermore, it is obvious that both figures follow the same pattern since they represent the same measure in a different scale.

Mode	new technique	KRAKEN-C
1	3.36634106e-01 + i3.81351852e-28	3.36634106e-01 + i2.91663806e-19
2	3.35720869e-01 + i4.50401142e-24	3.35720869e-01 + i1.41373053e-19
3	3.34947409e-01 + i1.84344990e-23	3.34947409e-01 + i4.18485568e-19
4	3.34163176e-01 + i1.54641986e-27	3.34163176e-01 + i7.31282998e-18
5	3.33342870e-01 + i6.34200193e-25	3.33342870e-01 + i1.89597338e-20
6	3.32530212e-01 + i1.65956018e-22	3.32530212e-01 + i3.36955521e-19
7	3.31736595e-01 + i3.41833159e-20	3.31736595e-01 + i2.95045279e-19
8	3.30951455e-01 + i4.74091728e-18	3.30951455e-01 + i4.48511153e-18
9	3.30186725e-01 + i4.35721259e-16	3.30186725e-01 + i4.35723924e-16
10	3.29444393e-01 + i2.67572596e-14	3.29444393e-01 + i2.67584947e-14

Table 5.12.: The first ten eigenvalues computed with the suggested technique and with KRAKEN-C for test case 5.2.3 with $f = 80\ Hz$

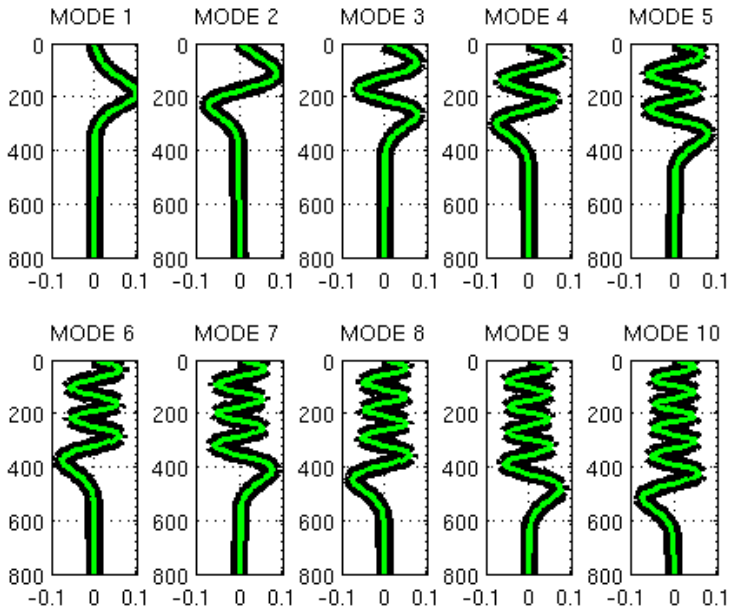

Figure 5.21.: Real part of the first ten eigenfunctions for test case 5.2.3 with $f = 80\ Hz$

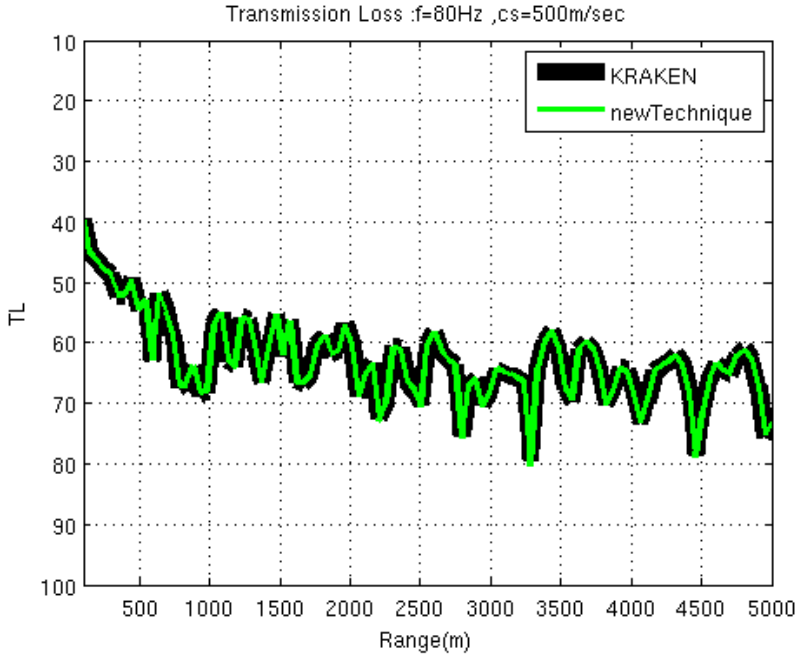

Figure 5.22.: Transmission loss calculated for test case 5.2.3 with $f = 80\ Hz$

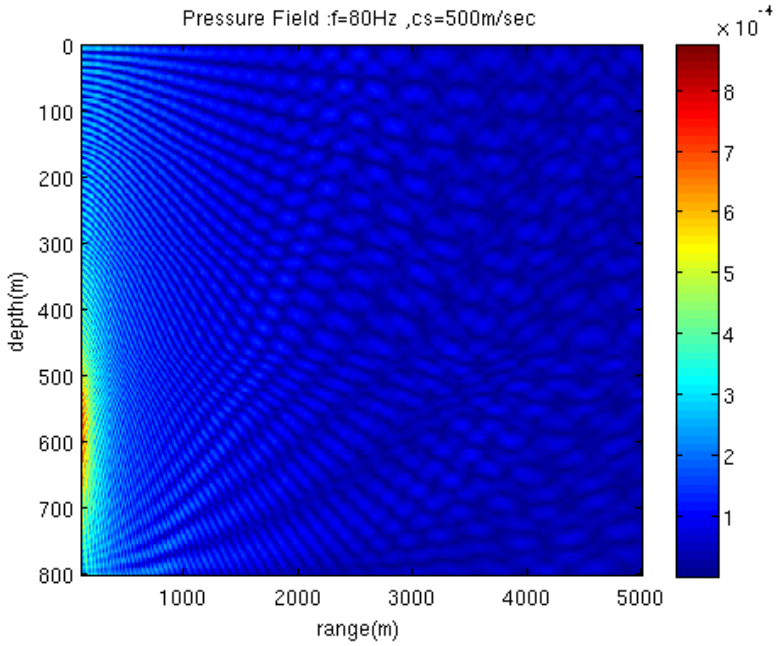

Figure 5.23.: Pressure field calculated in the whole domain $[0, 5000] \times [0, 500]$ for the test case 5.2.3 with $f = 80\ Hz$

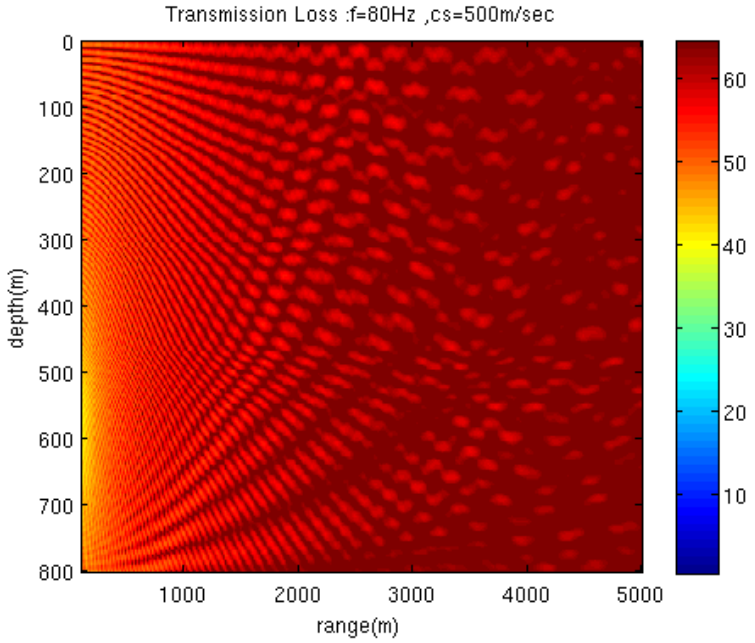

Figure 5.24.: Transmission loss calculated in the whole domain $[0, 5000] \times [0, 500]$ for the test case 5.2.3 with $f = 80\ Hz$

When the source frequency is 200 Hz

Indicatively, the first ten eigenvalues and the transmission loss for a greater frequency value have been included in this test case. The results, as calculated by our technique and the KRAKEN-C program, are presented in table 5.13 and figure 5.25. In order to this coincidence be achieved, in this case a much finer discretization was needed since the set of propagating modes is dense enough and consists of more than two hundred eigenvalues.

Mode	new technique	KRAKEN-C
1	8.42405903e-01 + i1.98705833e-26	8.42405903e-01 + i2.50362837e-18
2	8.41195771e-01 + i8.40194356e-24	8.41195771e-01 + i1.36908267e-18
3	8.40292563e-01 + i7.54343700e-38	8.40292563e-01 + i2.55175570e-18
4	8.39535101e-01 + i1.04496210e-24	8.39535101e-01 + i1.10057178e-18
5	8.38816595e-01 + i1.69237606e-24	8.38816595e-01 + i4.10620865e-18
6	8.38117544e-01 + i5.47936890e-36	8.38117544e-01 + i3.59878015e-19
7	8.37406925e-01 + i5.82653519e-35	8.37406925e-01 + i1.07700910e-18
8	8.36645906e-01 + i9.21599914e-32	8.36645906e-01 + i5.77774547e-19
9	8.35871071e-01 + i1.70795662e-25	8.35871071e-01 + i9.84544820e-19
10	8.35066890e-01 + i5.73386089e-34	8.35066890e-01 + i3.32593381e-19

Table 5.13.: The first ten eigenvalues computed with the suggested technique for test case 5.2.3 with $f = 200\ Hz$

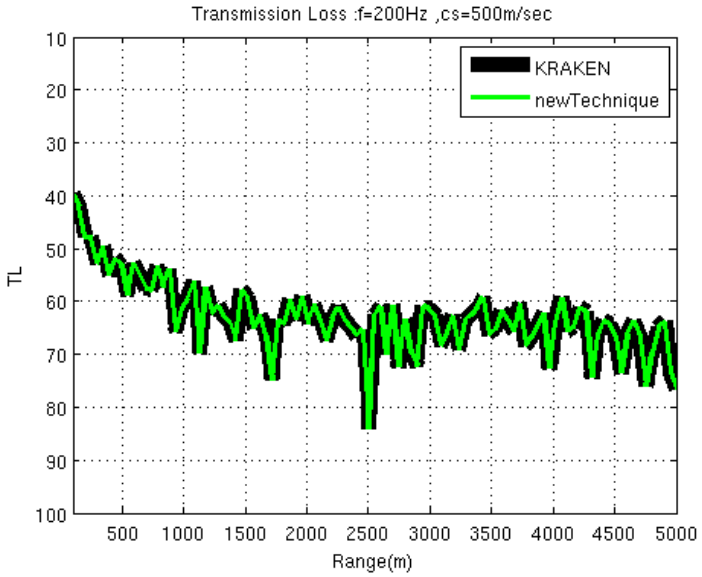

Figure 5.25.: Transmission loss calculated for test case 5.2.3 with $f = 200\ Hz$

In this chapter several test cases, for the suggested scheme, have been studied and the results were presented in comparison to those obtained by KRAKEN-C. The efficiency of the effective depth approach was presented first and various environmental scenarions were considered on which our iterative scheme was applied. The scheme was tested for various depths of the waveguide, sound speed profiles and for various values of the source frequency. In all cases the scheme appeared to converge with accuracy after less than ten iterations.

6. Summary - Conclusion

The problem of acoustic propagation in a shallow water range-independent environment has been presented. The associated "depth problem" both for a constant and a varying with depth velocity profile has been studied and the solution has been given in each case. A short description of the effective depth method has been presented for the calculation of the eigenvalues of the depth problem when the sound velocity is constant. In the case of a velocity profile varying with depth, a finite-difference scheme has been applied combined with the appropriate impedance function in the water-seabed interface and the discrete depth problem was formulated as a matrix eigenvalue problem.

An iterative procedure, based on Inverse Iteration method, has been suggested for the calculation of the eigenvalues in the varying velocity case. Initial assumptions for this procedure are obtained using the effective depth approach for a constant sound speed profile, corresponding to the minimum value of the actual profile. Several considerations have been taken into account to ensure that the scheme converges to the whole set of propagating modes.

In order to illustrate the efficiency of the suggested technique, several test cases have been studied and the results were compared to the output of the KRAKEN-C program. Eventually although we started on the purpose of approximating the eigenvalues, this technique came out to provide the eigenvalues with accuracy. Thus, it can be viewed as an alternative way to provide eigenvalues and eigenfunctions, for the series expansion of the acoustic field in a shallow water waveguide over an elastic homogeneous half-space.

Although our scheme has been shown to be efficient it appeared to be slow, particularly when the set of propagating modes is wide enough. As an issue of future study, one could apply parallel processing to minimize the execution time demanded. The estimation of eigenvalues corresponding to modes of different order, in practice corresponding to different initial assumptions, could be assigned to different threads leading to a reduced execution time. Also an issue could be that of implementing the suggested scheme for a multilayered seabed. Another issue for future research could concern the extention of the present iterative scheme to a range-dependend environment or an environment with non-horizontal boundaries. In such a problem further considerations would be needed in order to study the influence of this dependence on the acoustic field.

A. Derivation of pressure field and normalization constant

A.1. Pressure field

The solution to *Helmholtz* equation, by means of the spectral integral representation, is expressed as [10]

$$p(r,z) = \frac{1}{4\pi}\int_{-\infty}^{+\infty} G(z,z_0;\lambda)H_0^{(1)}(\lambda r)\lambda d\lambda \tag{A.1}$$

where $H_0^{(1)}$ is the *Hankel* function of the first kind of zeroth order and G is the Green's function which satisfies the inhomogeneous depth problem, for a constant density

$$\begin{gathered}\frac{d^2G}{dz^2} + (k^2(z) - \lambda_n^2)G = -\delta(z - z_0)\ ,\ z \in [0, D] \\ G(0) = 0 \\ \frac{G(D)}{G'(D)} = I(\lambda_n)\end{gathered}$$

The solution of the above problem is given as [1, 11]

$$G(z;\lambda) = -\frac{Z(z_0)V(z)}{W(z_0;\lambda)}\ ,\ z \in [0, z_0] \tag{A.2}$$

$$G(z;\lambda) = -\frac{Z(z)V(z_0)}{W(z_0;\lambda)}\ ,\ z \in [z_0, D] \tag{A.3}$$

where V and Z satisfy the top and bottom boundary conditions respectively and W denotes the Wronskian of U and V. That is,

$$W(z;\lambda) = V(z)Z'(z) - V'(z)Z(z) \tag{A.4}$$

and primes denote differentiation with respect to z.

Substitution of solution A.2 into expression A.1 and use of Cauchy's residue theorem for the poles λ_n of G, yields

$$p(r,z) = (-i2)\,\frac{1}{4}\sum_n \frac{Z_n(z_0)V_n(z)H_0^{(1)}(\lambda_n r)\lambda_n}{\partial W/\partial\lambda|_{\lambda=\lambda_n}}\ ,\ z \in [0, z_0] \tag{A.5}$$

where V_n and Z_n are associated with λ_n. The elimination of the coefficient of the sum has not been applied on purpose and the branch-line integrals have been neglected since

they have very small contribution at long ranges. Similar to A.5, substitution of A.3 into A.1, results in

$$p(r,z) = (-i2)\,\frac{1}{4}\sum_n \frac{V_n(z_0)Z_n(z)H_0^{(1)}(\lambda_n r)\lambda_n}{\partial W/\partial\lambda|_{\lambda=\lambda_n}}\ ,\ z\in[z_0,D]$$

Note that λ_n must satisfy

$$W(z_0;\lambda_n)=0$$

thus, V_n and Z_n are linearly dependent and, as such, they can be scaled so that they are equal. We set $U_n = V_n = Z_n$ and putting together the above expressions for the pressure field, we have

$$p(r,z) = \frac{i}{4}\sum_n \frac{U_n(z_0)U_n(z)H_0^{(1)}(\lambda_n r)}{\left.\frac{\partial W/\partial\lambda}{-2\lambda_n}\right|_{\lambda=\lambda_n}}\ ,\ z\in[0,D] \tag{A.6}$$

where U_n $(n = 1,2,3,\cdots)$ satisfy the homogeneous differential equation of the depth problem and both the top and bottom boundary conditions. Moreover, U_n are scaled so that

$$U_n(z) = N_n u_n(z)$$

where $N_n^2 = \left.\frac{\partial W/\partial\lambda}{-2\lambda_n}\right|_{\lambda=\lambda_n}$.

A.2. Normalization constant

We consider V, Z and U_n as above. Then V and U_n satisfy

$$\frac{d^2V}{dz^2} + (k^2(z)-\lambda^2)V = 0 \tag{A.7}$$

$$\frac{d^2U_n}{dz^2} + (k^2(z)-\lambda_n^2)U_n = 0 \tag{A.8}$$

respectively. We multiply A.7 by U_n, apply the operator $\int_0^D \cdot dz$ and multiply A.8 by V and integrate from 0 to D. If we integrate by parts and subtract the resulting expressions we obtain

$$\left[VU_n' - U_nV'\right]\Big|_0^D + (\lambda^2-\lambda_n^2)\int_0^D U_nV\,dz = 0 \tag{A.9}$$

Since the value of V at depth $z = D$ is not known, further considerations for $V(D)$ and $V'(D)$ are needed. The derivative of the Wronskian with respect to depth is

$$\begin{aligned} W'(z;\lambda) &= V'(z)Z'(z) + V(z)Z''(z) - V''(z)Z(z) - V'(z)Z'(z) \\ &= -V(z)(k^2(z)-\lambda^2)Z(z) + Z(z)(k^2(z)-\lambda^2)V(z) \\ &= 0 \end{aligned}$$

Thus,

$$W(z_0;\lambda) = W(D;\lambda) = V(D)Z'(D) - V'(D)Z(D)$$
$$\Leftrightarrow\ V'(D) = \frac{V(D)Z'(D)}{Z(D)} - \frac{W(z_0;\lambda)}{Z(D)} \tag{A.10}$$

Since U_n and Z satisfy $U_n'(D) = \frac{U_n(D)}{I(\lambda_n)}$ and $Z'(D) = \frac{Z(D)}{I(\lambda)}$ respectively, substitution of A.10 into the first term of A.9 gives

$$\left[VU_n' - U_nV'\right]\Big|_D = V(D)U_n(D)\left[\frac{1}{I(\lambda_n)} - \frac{1}{I(\lambda)}\right] + \frac{U_n(D)}{Z(D)}\left[W(z_0;\lambda) - W(z_0;\lambda_n)\right] \tag{A.11}$$

since $W(z_0;\lambda_n) = 0$. Additionally $\left[VU_n' - U_nV'\right]\Big|_0 = 0$ since $u_n(0) = V(0) = 0$. On substituting A.11 into A.9, dividing both sides by $\lambda - \lambda_n$ and reordering, we obtain

$$-\frac{U_n(D)}{Z(D)}\left[\frac{W(z_0;\lambda) - W(z_0;\lambda_n)}{\lambda - \lambda_n}\right] = (\lambda + \lambda_n)\int_0^D U_nV\,dz - V(D)U_n(D)\frac{I^{-1}(\lambda) - I^{-1}(\lambda)}{\lambda - \lambda_n}$$

As mentioned before, V can be scaled so that $V = U_n$ and still satisfy the corresponding differential equation. Moreover, we recall that both Z and U_n satisfy the boundary condition at $z = D$. Thus, if we scale V, take the limit as $\lambda \to \lambda_n$ and then divide by $2\lambda_n$ we have

$$-\frac{\partial W/\partial\lambda}{2\lambda_n}\Big|_{\lambda=\lambda_n} = \int_0^D U_n^2\,dz - \frac{U_n^2(D)}{2\lambda_n}\cdot\frac{dI^{-1}(\lambda)}{d\lambda}\Big|_{\lambda=\lambda_n} \tag{A.12}$$

which is desired result.

Bibliography

[1] H. P. Bucker, "Sound Propagation in a Channel with Lossy Boundaries, J. Acoust. Soc. Am. **48**, 1187-1194, (1970).

[2] M. B. Porter, E.L. Reiss, "A Numerical Model for Bottom Interacting Ocean Acoustic Normal Modes", J. Acoust. Soc. Am. **77**, 1760-1767 (1985)

[3] D.D. Ellis, D.M.F. Chapman, "A Simple Shallow Water Propagation Model Including Shear Wave Effects", J. Acoust. Soc. Am. **78**, 2087-2095, (1985).

[4] Z.Y. Zhang, C.T. Tindle, "Complex Effective Depth of the Ocean Bottom", J. Acoust. Soc. Am. **93**, 205-213 (1992).

[5] E.K. Westwood, C.T. Tindle, N.R. Chapman, "A Normal Mode Model for Acousto-Elastic Ocean Environments", J. Acoust. Soc. Am. **100**, 3631-3645 (1996).

[6] M. Καρινιωτακη, *Υπολογισμός του ακουστικού πεδίου σε ρηχό θαλάσσιο κυματοδηγό πάνω από ελαστικό πυθμένα*, Τμήμα Μαθηματικών Πανεπιστημίου Κρήτης, Μεταπτυχιακή εργασία (2004), (in Greek).

[7] G.H. Golub, C.F. Van Loan, *Matrix Computations*, 3rd edition, Johns Hopkins Univ. Press (1996).

[8] M. Taroudakis, G. Makrakis, "A Study of the Eigenvalues of the Depth Problem in Shallow Water Acoustic Propagation Modeling over an Elastic Halfspace", Proceedings of the Tenth International Congress on Sound and Vibration, Stockholm, Sweeden (2003).

[9] M. Taroudakis, I.Mastrokalos, "An Approximate Technique for Estimating Eigenvalues and Eigenfunctions of the Acoustic Field in Shallow Water over an Elastic Seabed", Proceedings of the Institute of Acoustics Congress on Seabed and Sediment Acoustics: Measurements and Modelling, Bath, United Kingdom (2015).

[10] K. Aki, P.G. Richards, *Quantitative Seismology*, 2nd edition, Univ. Science Books (2002).

[11] I. Stakgold, *Green's Functions and Boundary Value Problems*, Wiley (1979).